

WEAKLY-NORMAL BASIS VECTOR FIELDS IN RKHS WITH AN APPLICATION TO SHAPE NEWTON METHODS

ALBERTO PAGANINI ^{*} AND KEVIN STURM [†]

Abstract. We construct a space of vector fields that are normal to differentiable curves in the plane. Its basis functions are defined via saddle point variational problems in reproducing kernel Hilbert spaces (RKHSs). First, we study the properties of these basis vector fields and show how to approximate them. Then, we employ this basis to discretise shape Newton methods and investigate the impact of this discretisation on convergence rates.

Key words. shape optimisation, shape Newton method, numerical analysis, radial basis functions, reproducing kernel Hilbert spaces

AMS subject classifications. 49Q10, 49M15, 93B40, 65Dxx

1. Introduction. Shape optimisation is an active field of research that studies how to construct a shape Ω such that a shape functional J is minimised. An important tool to tackle shape optimisation problems are so-called shape derivatives.

Historically, shape derivatives [4, 11, 21] have been defined by flows of vector fields or by perturbations of the identity. More recently, Allaire et al. [1] have introduced an alternative definition of shape derivatives in terms of Hamilton-Jacobi equations, which coincides with previous derivatives when restricted to normal vector fields. The flow and perturbation of identity approach definitions lead to equivalent first derivatives but differing second ones [4]. However, not all second derivatives are suited to formulate shape Newton methods [17, 22].

Several papers propose Newton-type methods to specific PDE constrained problems with specific domain representations, e.g., star shaped domains; [7–9, 19, 20]. In [18], Schulz proves that, under certain assumptions, a Newton method formulated in shape spaces [15] converges quadratically, whereas superlinear convergence of a (discrete) shape Newton method in Micheletti spaces has been showed in [22]. In both papers, the authors have to tackle the problem of the shape Newton equation being well-posed only with respect to normal perturbations of the boundary.

In this paper, we introduce a new class of basis vector fields. We call these vector fields weakly-normal because they are solutions of saddle point variational problems in reproducing kernel Hilbert spaces (RKHSs). These variational problems ensure that the resulting vector fields are linearly independent and normal to the shape boundary $\partial\Omega$. Moreover, they form a dense subset of normal vector fields and can be used to formulate discrete shape Newton methods.

Similarly to [10], we work with the RKHS $[\mathcal{H}(\partial\Omega)]^2$ that is associated with restrictions of positive-definite kernels on \mathbf{R}^2 to the boundary $\partial\Omega$ of C^k , $k \geq 1$ domains $\Omega \subset \mathbf{R}^2$. For certain kernels, the corresponding RKHSs are classical boundary Sobolev spaces [23, Sec. 10]. Therefore, for these special kernels, our approach yields high order approximations of normal vector fields in boundary Sobolev spaces.

In this work, we restrict ourselves to the two dimensional case. We believe that the approach can be easily adapted to higher dimensions, but the implementation aspects may become more challenging.

^{*}Mathematical Institute, University of Oxford, Andrew Wiles Building, Radcliffe Observatory Quarter, Woodstock Road, Oxford, OX2 6GG. paganini@maths.ac.ox.uk

[†]Radon Institute for Computational and Applied Mathematics, Austrian Academy of Sciences, Altenberger Strasse 69, 4040 Linz, Austria, kevin.sturm@oeaw.ac.at

Structure of the paper. The paper is organised in two parts.

Section 2 deals with the formulation and the analysis of the proposed new class of normal vector fields. We study their properties, explain how to approximate them, and analyse the error of this approximation.

Section 3 deals with a shape Newton method and to its discretization with the basis functions introduced in **Section 2**. For a particular test case, we prove quasi-optimality of the approximate shape Newton update. Moreover, we examine numerically the impact of this approximation on the convergence rate of the optimization algorithm.

The theoretical results of this work are supported by numerical experiments performed in MATLAB and partly based on the Chebfun library [5].

2. Normal vector fields in RKHS.

2.1. RKHSs, Cartesian products, and trace spaces. We begin with some basic definitions of reproducing kernels.

DEFINITION 2.1. *Let $\mathcal{X} \subset \mathbf{R}^2$ be an arbitrary set. A function $k : \mathcal{X} \times \mathcal{X} \rightarrow \mathbf{R}$ is called reproducing kernel for the Hilbert space $\mathcal{H}(\mathcal{X})$ of functions $f : \mathcal{X} \rightarrow \mathbf{R}$, if*

- (a) $k(\mathbf{x}, \cdot) \in \mathcal{H}(\mathcal{X})$ for every $\mathbf{x} \in \mathcal{X}$,
- (b) $(k(\mathbf{x}, \cdot), f)_{\mathcal{H}} = f(\mathbf{x})$ for every $\mathbf{x} \in \mathcal{X}$ and every $f \in \mathcal{H}(\mathcal{X})$.

DEFINITION 2.2. *A kernel $k : \mathcal{X} \times \mathcal{X} \rightarrow \mathbf{R}$ is said to be positive-definite on \mathcal{X} if, for every finite subset of pairwise distinct points $\{\mathbf{x}_i\}_{i=1}^n \subset \mathcal{X}$, the matrix $(k(\mathbf{x}_i, \mathbf{x}_j))_{i,j=1}^n$ is positive-definite.*

DEFINITION 2.3. *A kernel $k : \mathcal{X} \times \mathcal{X} \rightarrow \mathbf{R}$ is said to be symmetric if*

$$k(\mathbf{x}, \mathbf{y}) = k(\mathbf{y}, \mathbf{x}) \quad \text{for all } \mathbf{x}, \mathbf{y} \in \mathcal{X}.$$

The main reason to consider symmetric positive-definite reproducing kernels is that they can be used to define certain Hilbert Spaces.

THEOREM 2.4. *To a positive-definite and symmetric kernel $k : \mathcal{X} \times \mathcal{X} \rightarrow \mathbf{R}$ defined on an arbitrary set $\mathcal{X} \subset \mathbf{R}^2$ corresponds a unique reproducing kernel Hilbert space $(\mathcal{H}(\mathcal{X}), (\cdot, \cdot)_{\mathcal{H}})$ (RKHS), which is called native space of k . Note that $(\cdot, \cdot)_{\mathcal{H}}$ depends on k .*

There is a variety of symmetric positive-definite reproducing kernels [23] (each tailored to specific applications). In this work, we are particularly interested in Wendland kernels with compact support, because compact support is a useful (and sometimes necessary [13]) feature for applications in shape optimisation. In the next example, we list three Wendland kernels and recall their native spaces.

EXAMPLE 2.5. *Classical examples of positive-definite kernels can be found in [23]. In this work, we are particularly interested in*

$$(1) \quad k_4^{\sigma}(x, y) := \left(1 - \frac{|x - y|}{\sigma}\right)_+^4 \left(4 \frac{|x - y|}{\sigma} + 1\right), \quad \sigma > 0,$$

where

$$(\cdot)_+ : \mathbf{R} \rightarrow \mathbf{R}_0^+, \quad x \mapsto (x)_+ := \max(0, x).$$

When $\sigma = 1$, (1) is the lowest order Wendland kernel with compact support that is positive-definite on \mathbf{R}^d (for $d \leq 3$) and is of class C^2 . When $\mathcal{X} = \mathbf{R}^2$, its native space

is $H^{2.5}(\mathbf{R}^2)$ [23, p. 160, Thm. 10.35]. When $\mathcal{X} = \Omega$ is a bounded smooth domain, its native space is $H^{2.5}(\Omega)$ (because every function $f \in \mathcal{H}(\Omega)$ can be extended to a function $\tilde{f} \in \mathcal{H}(\mathbf{R}^2) = H^{2.5}(\mathbf{R}^2)$ [23, p. 169, Thm. 10.46]). Similar properties can be proved for the C^4 -kernel k_6^σ and the C^6 -kernel k_8^σ , which are given by [23],

$$(2) \quad k_6^\sigma(x, y) := \frac{1}{3} \left(1 - \frac{|x - y|}{\sigma} \right)_+^6 \left(35 \frac{|x - y|^2}{\sigma^2} + 18 \frac{|x - y|}{\sigma} + 3 \right),$$

$$(3) \quad k_8^\sigma(x, y) := \left(1 - \frac{|x - y|}{\sigma} \right)_+^8 \left(32 \frac{|x - y|^3}{\sigma^3} + 25 \frac{|x - y|^2}{\sigma^2} + 8 \frac{|x - y|}{\sigma} + 1 \right),$$

respectively. Their corresponding native spaces in dimension two are $H^{3.5}(\mathbf{R}^2)$ and $H^{4.5}(\mathbf{R}^2)$, respectively [23, p. 160, Thm. 10.35].

Clearly, reproducing kernels can be used to define Hilbert spaces of vector valued functions, too [23].

PROPOSITION 2.6. *The Cartesian product $[\mathcal{H}(\mathcal{X})]^2 := \mathcal{H}(\mathcal{X}) \times \mathcal{H}(\mathcal{X})$ of a RKHS $\mathcal{H}(\mathcal{X})$ (with reproducing kernel k) is itself a RKHS. Its (matrix valued) reproducing kernel is $k(\cdot, \cdot)\mathbf{I}$, where $\mathbf{I} \in \mathbf{R}^2$ denotes the identity matrix.*

Next, we describe how to construct RKHSs on boundaries of bounded subdomains of \mathbf{R}^2 . Let k be a positive-definite kernel on \mathbf{R}^2 , and let $\mathcal{H}(\mathbf{R}^2)$ be its native space. Let $\Omega \subset \mathbf{R}^2$ be a nonempty, bounded, open and smooth set (e.g. C^1). We denote by ν and τ the unit normal and unit tangential vector fields along $\partial\Omega$.

The restriction of k onto $\partial\Omega$ defines a positive-definite kernel $k|_{\partial\Omega}$, which uniquely characterises the RKHS [23, p.169]

$$(4) \quad \mathcal{H}(\partial\Omega) = \{f|_{\partial\Omega} : f \in \mathcal{H}(\mathbf{R}^2)\}.$$

Similarly, it is possible to define the space of vector fields restricted onto $\partial\Omega$ by

$$(5) \quad [\mathcal{H}(\partial\Omega)]^2 = \{\mathbf{f}|_{\partial\Omega} : \mathbf{f} \in [\mathcal{H}(\mathbf{R}^2)]^2\}.$$

The next example identifies the space $\mathcal{H}(\partial\Omega)$ for the kernel (1).

EXAMPLE 2.7. *The native space of the restriction onto $\partial\Omega$ of the Wendland kernel k_4^σ (with σ fixed) is $H^2(\partial\Omega)$. This follows from $\mathcal{H}(\mathbf{R}^2) = H^{2.5}(\mathbf{R}^2)$ and the standard Sobolev trace theorem.*

We conclude this section by defining the RKHS of normal and tangential vector fields:

$$(6) \quad [\mathcal{H}(\partial\Omega)]_\nu^2 := \{\mathbf{f} \in [\mathcal{H}(\mathbf{R}^2)]^2 : \mathbf{f} \cdot \tau = 0 \quad \text{on } \partial\Omega\},$$

$$(7) \quad [\mathcal{H}(\partial\Omega)]_\tau^2 := \{\mathbf{f} \in [\mathcal{H}(\mathbf{R}^2)]^2 : \mathbf{f} \cdot \nu = 0 \quad \text{on } \partial\Omega\}.$$

2.2. Weakly-normal basis functions. In this section, we introduce a novel class of normal vector fields. We begin with the following assumption on the reproducing kernel k .

ASSUMPTION 2.8. *Let $k \geq 1$ be an integer and let $\partial\Omega$ be of class C^{k+1} . We assume that $k : \mathbf{R}^2 \times \mathbf{R}^2 \rightarrow \mathbf{R}$ is a symmetric positive-definite kernel on \mathbf{R}^2 with the property*

$$(8) \quad k(\mathbf{x}, \mathbf{x}) = 1 \quad \text{for all } \mathbf{x} \in \partial\Omega.$$

We assume that for every $\mathbf{x} \in \mathbf{R}^2$ we have $k(\mathbf{x}, \cdot) \in C^k(\mathbf{R}^2)$. Furthermore, we assume that there is a constant $c_\Omega > 0$, such that for every $\phi \in C^k(\partial\Omega)$ and every $f \in \mathcal{H}(\partial\Omega)$,

$$(9) \quad \phi f \in \mathcal{H}(\partial\Omega) \quad \text{and} \quad \|\phi f\|_{\mathcal{H}} \leq c_\Omega \|\phi\|_{C^k(\partial\Omega)} \|f\|_{\mathcal{H}}.$$

Finally, we assume that the identity map $1 : \partial\Omega \rightarrow \partial\Omega$ belongs to $[\mathcal{H}(\partial\Omega)]^2$ and, for simplicity, that the support of k is connected.

EXAMPLE 2.9. The kernels k_4^σ, k_6^σ and k_8^σ satisfy [Assumption 2.8](#) for $k = 2, 3, 4$, respectively.

REMARK 2.10. Property (9) implies that $C^k(\partial\Omega) \subset \mathcal{H}(\partial\Omega)$ (by (9)), and that $[\mathcal{H}(\partial\Omega)]^2 = [\mathcal{H}(\partial\Omega)]_\nu^2 \oplus [\mathcal{H}(\partial\Omega)]_\tau^2$ (because every vector field $\mathbf{v} \in [\mathcal{H}(\partial\Omega)]^2$ can be decomposed into $\mathbf{v} = (\mathbf{v} \cdot \boldsymbol{\nu})\boldsymbol{\nu} + (\mathbf{v} \cdot \boldsymbol{\tau})\boldsymbol{\tau}$ on $\partial\Omega$).

DEFINITION 2.11. For a point $\mathbf{x} \in \partial\Omega$, let $(\mathbf{r}_\mathbf{x}, p_\mathbf{x}) \in [\mathcal{H}(\partial\Omega)]^2 \times \mathcal{H}(\partial\Omega)$ be the solution of

$$(10a) \quad (\mathbf{r}_\mathbf{x}, \boldsymbol{\varphi})_{[\mathcal{H}]^2} + (\boldsymbol{\varphi} \cdot \boldsymbol{\tau}, p_\mathbf{x})_{\mathcal{H}} = \boldsymbol{\nu}(\mathbf{x}) \cdot \boldsymbol{\varphi}(\mathbf{x}) \quad \text{for all } \boldsymbol{\varphi} \in [\mathcal{H}(\partial\Omega)]^2,$$

$$(10b) \quad (\mathbf{r}_\mathbf{x} \cdot \boldsymbol{\tau}, \psi)_{\mathcal{H}} = 0 \quad \text{for all } \psi \in \mathcal{H}(\partial\Omega).$$

The function $\mathbf{r}_\mathbf{x}$ is the weakly-normal basis function associated with \mathbf{x} .

[Lemma 2.13](#) shows that [Definition 2.11](#) makes sense. The proof of [Lemma 2.13](#) relies on [Lemma 2.12](#). Henceforth, we denote by $\mathbf{e}_i, i = 1, 2$, the canonical basis of \mathbf{R}^2 and use the norm

$$(11) \quad \|\mathbf{f}\|_{C^k} := \sqrt{\|\mathbf{f} \cdot \mathbf{e}_1\|_{C^k}^2 + \|\mathbf{f} \cdot \mathbf{e}_2\|_{C^k}^2} \quad \text{for all } \mathbf{f} \in C^k(\mathbf{R}^2, \mathbf{R}^2).$$

LEMMA 2.12. The operator $B : [\mathcal{H}(\partial\Omega)]^2 \rightarrow \mathcal{H}(\partial\Omega)^*$ defined by $\boldsymbol{\varphi} \mapsto (\boldsymbol{\varphi} \cdot \boldsymbol{\tau}, \cdot)_{\mathcal{H}}$ is surjective. Moreover,

$$(12) \quad \|B^* \psi\|_{\mathcal{H}^*} \geq \frac{\|\psi\|_{\mathcal{H}}}{c_\Omega \|\boldsymbol{\tau}\|_{C^k}} \quad \text{for all } \psi \in \mathcal{H}(\partial\Omega).$$

Proof. Let $f \in \mathcal{H}(\partial\Omega)^*$. By the Riesz representation theorem, there is a function $\eta_f \in \mathcal{H}(\partial\Omega)$ that satisfies $f(\psi) = (\eta_f, \psi)_{\mathcal{H}}$ for all $\psi \in \mathcal{H}(\partial\Omega)$. Since the function $\boldsymbol{\varphi} := \eta_f \boldsymbol{\tau} \in [\mathcal{H}(\partial\Omega)]^2$ satisfies $B\boldsymbol{\varphi} = f$, B is surjective. To verify (12), first note that inequality (9) implies $\|\boldsymbol{\tau}\psi\|_{[\mathcal{H}]^2} \leq c_\Omega \|\boldsymbol{\tau}\|_{C^k} \|\psi\|_{\mathcal{H}}$ for every $\psi \in \mathcal{H}(\partial\Omega)$. Thus,

$$\|B^* \psi\|_{\mathcal{H}^*} = \sup_{\substack{\boldsymbol{\varphi} \in [\mathcal{H}(\partial\Omega)]^2 \\ \|\boldsymbol{\varphi}\|_{[\mathcal{H}]^2} = 1}} |(\boldsymbol{\varphi} \cdot \boldsymbol{\tau}, \psi)_{\mathcal{H}}| \geq \left(\boldsymbol{\tau} \cdot \frac{(\boldsymbol{\tau}\psi)}{\|\boldsymbol{\tau}\psi\|_{[\mathcal{H}]^2}}, \psi \right)_{\mathcal{H}} = \frac{\|\psi\|_{\mathcal{H}}^2}{\|\boldsymbol{\tau}\psi\|_{[\mathcal{H}]^2}} \geq \frac{\|\psi\|_{\mathcal{H}}}{c_\Omega \|\boldsymbol{\tau}\|_{C^k}}. \quad \square$$

LEMMA 2.13. Let $\mathbf{x} \in \partial\Omega$. The saddle point problem (10) admits a unique solution, which satisfies

$$(13) \quad \|\mathbf{r}_\mathbf{x}\|_{[\mathcal{H}]^2} \leq \frac{1}{\|\boldsymbol{\nu}\|_{[\mathcal{H}]^2}}, \quad \text{and} \quad \|p_\mathbf{x}\|_{\mathcal{H}} \leq \frac{2c_\Omega \|\boldsymbol{\tau}\|_{C^k}}{\|\boldsymbol{\nu}\|_{[\mathcal{H}]^2}}.$$

Proof. Since B is surjective and $(\cdot, \cdot)_{[\mathcal{H}]^2}$ is an inner product, existence and uniqueness follow from the classical result [2, Thm 4.2.1, p.224]. The continuity estimates (13) follow from [2, Thm 4.2.3, p.228], (12), and the estimate

$$(14) \quad \sup_{\substack{\boldsymbol{\varphi} \in [\mathcal{H}]^2, \\ \|\boldsymbol{\varphi}\|_{[\mathcal{H}]^2} = 1}} |\boldsymbol{\nu}(\mathbf{x}) \cdot \boldsymbol{\varphi}(\mathbf{x})| \leq \frac{|\boldsymbol{\nu}(\mathbf{x}) \cdot \boldsymbol{\nu}(\mathbf{x})|}{\|\boldsymbol{\nu}\|_{[\mathcal{H}]^2}} \leq 1/\|\boldsymbol{\nu}\|_{[\mathcal{H}]^2}. \quad \square$$

The following remark provides an alternative definition of the function \mathbf{r}_x .

REMARK 2.14. *Let $\mathbf{x} \in \partial\Omega$. The solution $\mathbf{r}_x \in [\mathcal{H}(\partial\Omega)]^2$ of (10) is the unique minimiser of*

$$(15) \quad \min_{\substack{\varphi \in [\mathcal{H}(\partial\Omega)]^2, \\ \varphi \cdot \boldsymbol{\tau} = 0 \text{ on } \partial\Omega}} \frac{1}{2} \|\varphi\|_{[\mathcal{H}]^2}^2 - \boldsymbol{\nu}(\mathbf{x}) \cdot \varphi(\mathbf{x}).$$

Proof. By differentiating the Lagrangian functional

$$(16) \quad \mathcal{L} : [\mathcal{H}(\partial\Omega)]^2 \times \mathcal{H}(\partial\Omega) \rightarrow \mathbf{R}, \quad (\varphi, \psi) \mapsto \frac{1}{2} \|\varphi\|_{[\mathcal{H}]^2}^2 - \boldsymbol{\nu}(\mathbf{x}) \cdot \varphi(\mathbf{x}) + (\varphi \cdot \boldsymbol{\tau}, \psi)_{\mathcal{H}},$$

it is easy to see that equations (10) are the first order optimality conditions of (15). This is the so-called Lagrange multiplier rule. Since $\varphi \mapsto 1/2\|\varphi\|_{[\mathcal{H}]^2}^2 - \boldsymbol{\nu}(\mathbf{x}) \cdot \varphi(\mathbf{x})$ is a convex and coercive functional, \mathbf{r}_x is a minimiser of (15), where (\mathbf{r}_x, p_x) is a solution of the saddle point equation (10). \square

In the next theorem, we analyse in details the properties of \mathbf{r}_x and show that, in general, \mathbf{r}_x is neither $\boldsymbol{\nu}(\cdot)k(\mathbf{x}, \cdot)$ nor $\boldsymbol{\nu}(\cdot)$. To facilitate the interpretation, in Figure 1 we include some plots of the function \mathbf{r}_x .

THEOREM 2.15. *Let $\mathbf{x} \in \partial\Omega$. The solution (\mathbf{r}_x, p_x) of (10) has the following properties.*

- (a) $\mathbf{r}_x \in [\mathcal{H}(\partial\Omega)]_{\boldsymbol{\nu}}^2$.
- (b) $\|\mathbf{r}_x\|_{[\mathcal{H}]^2} \leq 1$.
- (c) $\|\mathbf{r}_x\|_{[\mathcal{H}]^2} > 0$, and the surface measure of $\text{supp}(\mathbf{r}_x)$ is strictly greater than zero.
- (d) The equality $\|\mathbf{r}_x\|_{[\mathcal{H}]^2} = 1$ holds if and only if $\partial\Omega \cap \text{supp}(\mathbf{r}_x)$ is a straight segment. In particular, $(\mathbf{r}_x, p_x) = (k(\mathbf{x}, \cdot)\boldsymbol{\nu}(\mathbf{x}), 0)$.
- (e) $(\mathbf{r}_x, \boldsymbol{\nu})_{[\mathcal{H}]^2} = 1$ and $\|\boldsymbol{\nu}\|_{[\mathcal{H}]^2} \|\mathbf{r}_x\|_{[\mathcal{H}]^2} = 1$. In particular, if $\|\boldsymbol{\nu}\|_{[\mathcal{H}]^2} = 1$, then $\partial\Omega$ is a straight segment.
- (f) If $\partial\Omega \cap \text{supp}(\mathbf{r}_x)$ is not a straight segment, then

$$(17) \quad \mathbf{r}_x \neq \boldsymbol{\nu}(\cdot)k(\mathbf{x}, \cdot) \quad \text{and} \quad \mathbf{r}_x \neq \boldsymbol{\nu}.$$

- (g) The basis functions $\mathbf{r}_x, \mathbf{r}_y$ associated with the points $\mathbf{x}, \mathbf{y} \in \partial\Omega$ satisfy

$$(18) \quad \mathbf{r}_x(\mathbf{y}) \cdot \boldsymbol{\nu}(\mathbf{y}) = \mathbf{r}_y(\mathbf{x}) \cdot \boldsymbol{\nu}(\mathbf{x}).$$

Moreover, for each $\mathbf{x} \in \partial\Omega$ there is a neighborhood U_x of \mathbf{x} such that $\mathbf{r}_x(\mathbf{y}) \cdot \boldsymbol{\nu}(\mathbf{y}) > 0$ for all $\mathbf{y} \in U_x$.

Proof. Item a follows from (10b), because $\mathbf{r}_x(\mathbf{y}) \cdot \boldsymbol{\tau}(\mathbf{y}) = (\mathbf{r}_x \cdot \boldsymbol{\tau}, k(\mathbf{y}, \cdot))_{\mathcal{H}} = 0$ for every $\mathbf{y} \in \partial\Omega$.

To show Item b, note that choosing $\varphi = \mathbf{r}_x$ in (10a) gives

$$(19) \quad \|\mathbf{r}_x\|_{[\mathcal{H}]^2}^2 = \mathbf{r}_x(\mathbf{x}) \cdot \boldsymbol{\nu}(\mathbf{x}) \leq |\mathbf{r}_x(\mathbf{x})| = \sqrt{|\mathbf{r}_x(\mathbf{x}) \cdot \mathbf{e}_1|^2 + |\mathbf{r}_x(\mathbf{x}) \cdot \mathbf{e}_2|^2}.$$

The reproducing kernel property of k and (8) imply

$$(20) \quad \|k(\mathbf{x}, \cdot)\|_{\mathcal{H}}^2 = (k(\mathbf{x}, \cdot), k(\mathbf{x}, \cdot))_{\mathcal{H}} = k(\mathbf{x}, \mathbf{x}) = 1.$$

Therefore, by the reproducing kernel property of k and Cauchy-Schwarz inequality,

$$(21) \quad |\mathbf{r}_x(\mathbf{x}) \cdot \mathbf{e}_i| = |(k(\mathbf{x}, \cdot), \mathbf{r}_x \cdot \mathbf{e}_i)_{\mathcal{H}}| \leq \|k(\mathbf{x}, \cdot)\|_{\mathcal{H}} \|\mathbf{r}_x \cdot \mathbf{e}_i\|_{\mathcal{H}} = \|\mathbf{r}_x \cdot \mathbf{e}_i\|_{\mathcal{H}},$$

and thus,

$$|\mathbf{r}_x(\mathbf{x})|^2 = |\mathbf{r}_x(\mathbf{x}) \cdot \mathbf{e}_1|^2 + |\mathbf{r}_x(\mathbf{x}) \cdot \mathbf{e}_2|^2 \leq \|\mathbf{r}_x \cdot \mathbf{e}_1\|_{\mathcal{H}}^2 + \|\mathbf{r}_x \cdot \mathbf{e}_2\|_{\mathcal{H}}^2 = \|\mathbf{r}_x\|_{[\mathcal{H}]^2}^2.$$

In light of (19), this yields

$$(22) \quad \|\mathbf{r}_x\|_{[\mathcal{H}]^2}^2 \leq |\mathbf{r}_x(\mathbf{x})| \leq \|\mathbf{r}_x\|_{[\mathcal{H}]^2},$$

which, in turn, implies $\|\mathbf{r}_x\|_{[\mathcal{H}]^2} \leq 1$.

To show Item c, suppose that $\mathbf{r}_x = 0$. Then, $p_x = 0$, because (10a) implies that for any $\mathbf{y} \in \partial\Omega$

$$\begin{aligned} p_x(\mathbf{y}) &= (\mathbf{k}(\mathbf{y}, \cdot), p_x)_{\mathcal{H}} = (\mathbf{k}(\mathbf{y}, \cdot) \boldsymbol{\tau}(\cdot) \cdot \boldsymbol{\tau}(\cdot), p_x)_{\mathcal{H}} \\ &= \boldsymbol{\nu}(\mathbf{x}) \cdot \mathbf{k}(\mathbf{y}, \mathbf{x}) \boldsymbol{\tau}(\mathbf{x}) - (\mathbf{r}_x, \mathbf{k}(\mathbf{y}, \cdot) \boldsymbol{\tau}(\cdot))_{[\mathcal{H}]^2} = 0. \end{aligned}$$

However, $(\mathbf{r}_x, p_x) = 0$ does not satisfy (10a) when the test function $\boldsymbol{\varphi}$ is $\boldsymbol{\varphi} = \mathbf{k}(\mathbf{x}, \cdot) \boldsymbol{\nu}(\cdot) \in [\mathcal{H}(\partial\Omega)]^2$. Finally, $\mathbf{r}_x \neq 0$ implies that there is at least a point $\mathbf{y} \in \partial\Omega$ such that $\mathbf{r}_x(\mathbf{y}) \neq 0$. Since \mathbf{r}_x is continuous on $\partial\Omega$, $\text{supp}(\mathbf{r}_x)$ contains an nonempty neighborhood $U_{\mathbf{y}}$ of \mathbf{y} .

To show Item d, let us first assume that $\|\mathbf{r}_x\|_{[\mathcal{H}]^2} = 1$. Then, equation (22) implies $|\mathbf{r}_x(\mathbf{x})| = \|\mathbf{r}_x\|_{[\mathcal{H}]^2}$, and since

$$|\mathbf{r}_x(\mathbf{x}) \cdot \mathbf{e}_1|^2 + |\mathbf{r}_x(\mathbf{x}) \cdot \mathbf{e}_2|^2 = |\mathbf{r}_x(\mathbf{x})|^2 = \|\mathbf{r}_x\|_{[\mathcal{H}]^2}^2 = \|\mathbf{r}_x \cdot \mathbf{e}_1\|_{\mathcal{H}}^2 + \|\mathbf{r}_x \cdot \mathbf{e}_2\|_{\mathcal{H}}^2,$$

equation (21) becomes an equality (because $|\mathbf{r}_x(\mathbf{x}) \cdot \mathbf{e}_i| \leq \|\mathbf{r}_x \cdot \mathbf{e}_i\|_{\mathcal{H}}$). In particular, this implies that

$$|(\mathbf{k}(\mathbf{x}, \cdot), \mathbf{r}_x \cdot \mathbf{e}_i)_{\mathcal{H}}| = \|\mathbf{k}(\mathbf{x}, \cdot)\|_{\mathcal{H}} \|\mathbf{r}_x \cdot \mathbf{e}_i\|_{\mathcal{H}}.$$

For nonzero vectors, Cauchy-Schwarz inequality becomes an equality if and only if the two vectors are linearly dependent. Since $\mathbf{k}(\mathbf{x}, \cdot)$ and \mathbf{r}_x are both nonzero, there is a nonzero vector $\boldsymbol{\alpha} \in \mathbf{R}^2$ such that $\mathbf{r}_x(\cdot) = \mathbf{k}(\mathbf{x}, \cdot) \boldsymbol{\alpha}$ (in fact, $|\boldsymbol{\alpha}| = 1$ because $|\mathbf{r}_x(\mathbf{x})| = 1 = \|\mathbf{k}(\mathbf{x}, \mathbf{x})\|$). This, combined with $\mathbf{r}_x \in [\mathcal{H}(\partial\Omega)]_{\boldsymbol{\nu}}^2$ (see Item a), implies that $\boldsymbol{\nu}$ restricted to $\partial\Omega \cap \text{supp}(\mathbf{k}(\mathbf{x}, \cdot))$ is either $\boldsymbol{\alpha}$ or $-\boldsymbol{\alpha}$, and thus constant.

On the other hand, note that

$$(\mathbf{k}(\mathbf{x}, \cdot) \boldsymbol{\nu}(\mathbf{x}), \boldsymbol{\varphi})_{[\mathcal{H}]^2} = \boldsymbol{\nu}(\mathbf{x}) \cdot \mathbf{e}_1 (\mathbf{k}(\mathbf{x}, \cdot), \boldsymbol{\varphi} \cdot \mathbf{e}_1)_{\mathcal{H}} + \boldsymbol{\nu}(\mathbf{x}) \cdot \mathbf{e}_2 (\mathbf{k}(\mathbf{x}, \cdot), \boldsymbol{\varphi} \cdot \mathbf{e}_2)_{\mathcal{H}} = \boldsymbol{\nu}(\mathbf{x}) \cdot \boldsymbol{\varphi}(\mathbf{x}),$$

which implies that $(\mathbf{r}_x, p_x) = (\mathbf{k}(\mathbf{x}, \cdot) \boldsymbol{\nu}(\mathbf{x}), 0)$ satisfies (10a). If $\partial\Omega \cap \text{supp}(\mathbf{r}_x)$ is a straight segments, then $\boldsymbol{\nu}(\mathbf{x}) \cdot \boldsymbol{\tau}(\mathbf{y}) = 0$ for all $\mathbf{y} \in \partial\Omega \cap \text{supp}(\mathbf{k}(\mathbf{x}, \cdot))$. Since $\mathbf{k}(\mathbf{x}, \mathbf{y}) = 0$ for all $\mathbf{y} \notin \text{supp}(\mathbf{k}(\mathbf{x}, \cdot))$,

$$(\mathbf{k}(\mathbf{x}, \cdot) \boldsymbol{\nu}(\mathbf{x}) \cdot \boldsymbol{\tau}(\cdot), \mathbf{k}(\mathbf{y}, \cdot))_{\mathcal{H}} = \mathbf{k}(\mathbf{x}, \mathbf{y}) \boldsymbol{\nu}(\mathbf{x}) \cdot \boldsymbol{\tau}(\mathbf{y}) = 0 \quad \text{for every } \mathbf{y} \in \partial\Omega,$$

and Equation (10b) is also satisfied. Finally, $\|\mathbf{k}(\mathbf{x}, \cdot) \boldsymbol{\nu}(\mathbf{x})\|_{[\mathcal{H}]^2}^2 = |\boldsymbol{\nu}(\mathbf{x})|^2 \|\mathbf{k}(\mathbf{x}, \cdot)\|_{\mathcal{H}}^2 = 1$ by (20).

To show Item e, recall that $1 \in [\mathcal{H}(\partial\Omega)]^2$ by Assumption 2.8. Therefore, $\boldsymbol{\nu} \in [\mathcal{H}(\partial\Omega)]^2$, and replacing by $\boldsymbol{\varphi} = \boldsymbol{\nu}$ in (10a) shows that $(\mathbf{r}_x, \boldsymbol{\nu})_{[\mathcal{H}]^2} = 1$. So, by Cauchy-Schwarz inequality and (13),

$$(23) \quad 1 = (\mathbf{r}_x, \boldsymbol{\nu})_{[\mathcal{H}]^2} \leq \|\boldsymbol{\nu}\|_{[\mathcal{H}]^2} \|\mathbf{r}_x\|_{[\mathcal{H}]^2} \leq 1.$$

Moreover, if $\|\nu\|_{[\mathcal{H}]^2} = 1$, then $\|\mathbf{r}_x\|_{[\mathcal{H}]^2} = 1$ for every $\mathbf{x} \in \partial\Omega$. By [Item d](#), it follows that $\partial\Omega \cap \text{supp}(\mathbf{r}_x)$ is a straight segment. Since this is the case for every $\mathbf{x} \in \partial\Omega$, it follows that $\partial\Omega$ is a straight segment itself.

To show [Item f](#), let $\mathbf{y} \in \partial\Omega$. Plugging $\nu(\cdot)\mathbf{k}(\mathbf{y}, \cdot)$ into [\(10a\)](#) shows that

$$(24) \quad (\mathbf{r}_x, \nu(\cdot)\mathbf{k}(\mathbf{y}, \cdot))_{[\mathcal{H}]^2} = \mathbf{k}(\mathbf{x}, \mathbf{y}).$$

In particular, $(\mathbf{r}_x, \nu(\cdot)\mathbf{k}(\mathbf{x}, \cdot))_{[\mathcal{H}]^2} = \mathbf{k}(\mathbf{x}, \mathbf{x}) = 1$. Therefore,

$$(25) \quad 0 \leq \|\mathbf{r}_x - \nu(\cdot)\mathbf{k}(\mathbf{x}, \cdot)\|_{[\mathcal{H}]^2}^2 = \|\mathbf{r}_x\|_{[\mathcal{H}]^2}^2 + \|\nu(\cdot)\mathbf{k}(\mathbf{x}, \cdot)\|_{[\mathcal{H}]^2}^2 - 2$$

$$(26) \quad = (\|\mathbf{r}_x\|_{[\mathcal{H}]^2}^2 - 1) + (\|\nu(\cdot)\mathbf{k}(\mathbf{x}, \cdot)\|_{[\mathcal{H}]^2}^2 - 1).$$

Since [Item d](#) implies that $\|\mathbf{r}_x\|_{[\mathcal{H}]^2} < 1$, we conclude that $\|\nu(\cdot)\mathbf{k}(\mathbf{x}, \cdot)\|_{[\mathcal{H}]^2} > 1$, and $\mathbf{r}_x \neq \nu(\cdot)\mathbf{k}(\mathbf{x}, \cdot)$. Finally, [Item e](#) states that $(\mathbf{r}_x, \nu)_{[\mathcal{H}]^2} = 1$. Therefore,

$$(27) \quad 0 \leq \|\mathbf{r}_x - \nu\|_{[\mathcal{H}]^2}^2 = (\|\mathbf{r}_x\|_{[\mathcal{H}]^2}^2 - 1) + (\|\nu\|_{[\mathcal{H}]^2}^2 - 1),$$

and $\mathbf{r}_x \neq \nu$ because $\|\nu\|_{[\mathcal{H}]^2} > 1$.

To show [Item g](#), note that $(\mathbf{r}_x, \mathbf{r}_y)_{[\mathcal{H}]^2} = (\mathbf{r}_y, \mathbf{r}_x)_{[\mathcal{H}]^2}$. Therefore, by [\(10a\)](#),

$$(28) \quad \nu(\mathbf{x}) \cdot \mathbf{r}_y(\mathbf{x}) = (\mathbf{r}_x, \mathbf{r}_y)_{[\mathcal{H}]^2} = (\mathbf{r}_y, \mathbf{r}_x)_{[\mathcal{H}]^2} = \nu(\mathbf{y}) \cdot \mathbf{r}_x(\mathbf{y}).$$

For $\mathbf{x} = \mathbf{y}$, this implies $\mathbf{r}_x(\mathbf{x}) \cdot \nu(\mathbf{x}) = \|\mathbf{r}_x\|_{[\mathcal{H}]^2}^2 > 0$. Since $\mathbf{y} \mapsto \mathbf{r}_x(\mathbf{y}) \cdot \nu(\mathbf{y})$ is continuous, there is a neighborhood U_x of \mathbf{x} such $\mathbf{r}_x(\mathbf{y}) \cdot \nu(\mathbf{y}) > 0$ for all $\mathbf{y} \in U_x$. \square

REMARK 2.16. *The vector field \mathbf{r}_x depends on the metric induced by the kernel \mathbf{k} . For instance, varying the parameters of the Wendland-kernel [\(1\)](#) results in different \mathbf{r}_x s; see [Figure 1](#). In particular, we observe that the decay of \mathbf{r}_x away from \mathbf{x} is influenced by the support of the kernel k_p^σ .*

2.3. Density of weakly-normal functions. In this section we study the approximation properties of the functions \mathbf{r}_x s with respect to $[\mathcal{H}(\partial\Omega)]_\nu^2$.

Let $N \geq 1$ be an integer and let $\mathcal{X}_N := \{\mathbf{x}_1, \dots, \mathbf{x}_N\} \subset \partial\Omega$ be a collection of pairwise distinct points.

LEMMA 2.17. *The functions $\mathbf{r}_{\mathbf{x}_1}, \dots, \mathbf{r}_{\mathbf{x}_N}$ associated with the points in \mathcal{X}_N are linearly independent.*

Proof. Let $\gamma_1, \dots, \gamma_N \in \mathbf{R}$ be such that $\mathbf{r} := \sum_{i=1}^N \gamma_i \mathbf{r}_{\mathbf{x}_i} = 0$. Setting $p := \sum_{i=1}^N \gamma_i p_{\mathbf{x}_i}$ and summing [\(10a\)](#) over $i = 1, \dots, N$ yields

$$(29) \quad (\varphi \cdot \tau, p)_\mathcal{H} = \sum_{i=1}^N \gamma_i \nu(\mathbf{x}_i) \cdot \varphi(\mathbf{x}_i) = \left(\sum_{i=1}^N \gamma_i \mathbf{k}(\mathbf{x}_i, \cdot), \nu \cdot \varphi \right)_\mathcal{H} \quad \text{for all } \varphi \in [\mathcal{H}(\partial\Omega)]^2.$$

Choosing $\varphi = (\sum_{i=1}^N \gamma_i k(\mathbf{x}_i, \cdot))\nu \in [\mathcal{H}(\partial\Omega)]_\nu^2$ (cf. [Assumption 2.8](#)), yields

$$(30) \quad \left\| \sum_{i=1}^N \gamma_i \mathbf{k}(\mathbf{x}_i, \cdot) \right\|_{\mathcal{H}}^2 = 0, \quad \text{and thus,} \quad \sum_{i=1}^N \gamma_i \mathbf{k}(\mathbf{x}_i, \mathbf{y}) = 0 \quad \text{for all } \mathbf{y} \in \mathbf{R}^2.$$

In particular, this implies that

$$(31) \quad \sum_{i=1}^N \gamma_i \mathbf{k}(\mathbf{x}_i, \mathbf{x}_j) = 0 \quad \text{for all } \mathbf{x}_j \in \mathcal{X}_N,$$

and thus, $\gamma_1 = \dots = \gamma_N = 0$, because \mathbf{k} is positive-definite on \mathbf{R}^2 . Therefore, the functions $\mathbf{r}_{\mathbf{x}_1}, \dots, \mathbf{r}_{\mathbf{x}_N}$ are linearly independent. \square

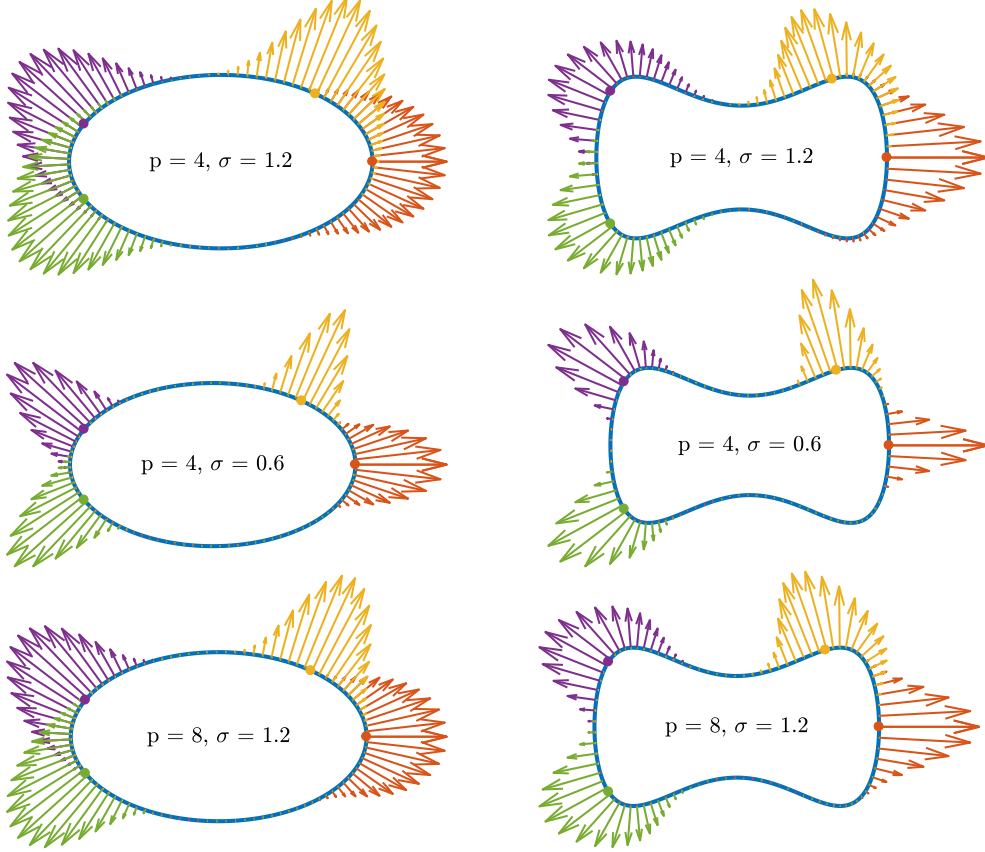


FIG. 1. Some weakly-normal basis functions based on compactly supported Wendland kernels (1) and (3) when $\partial\Omega$ is the ellipse $\{\gamma(\phi) = (1.4\cos(\phi), 0.8\sin(\phi)) : \phi \in [0, 2\pi]\}$ (left) and the nonconvex domain $\{\gamma(\phi) = (1.4\cos(\phi), 0.8\sin(\phi) + 0.3\sin(3\phi)) : \phi \in [0, 2\pi]\}$ (right). The dots denote the points to which the weakly-normal basis functions are associated with. We observe that different choices of kernel parameters result in different weakly-normal basis functions.

Lemma 2.17 allows the definition of the interpolation operator onto $\mathcal{R}_N := \text{span}\{\mathbf{r}_x : x \in \mathcal{X}_N\}$. The following lemma and remark clarify the approximation properties of \mathcal{R}_N on $[\mathcal{H}(\partial\Omega)]^2$.

LEMMA 2.18. *The interpolation operator $[\mathcal{H}(\partial\Omega)]_\nu^2 \ni \mathbf{r} \mapsto \mathbf{r}_N \in \mathcal{R}_N$, defined by*

$$(32) \quad \mathbf{r}(\mathbf{x}) = \mathbf{r}_N(\mathbf{x}) \quad \text{for every } \mathbf{x} \in \mathcal{X}_N$$

is an $[\mathcal{H}]^2$ -orthogonal projection.

Proof. First of all, recall that $\mathbf{r}_x \in [\mathcal{H}(\partial\Omega)]_\nu^2$ for every $\mathbf{x} \in \mathcal{X}_N$. Therefore, $\mathbf{r}_N \in [\mathcal{H}(\partial\Omega)]_\nu^2$. For $\mathbf{x} \in \mathcal{X}_N$ fixed, using \mathbf{r} and \mathbf{r}_N as a test functions in (10a) gives

$$(33) \quad (\mathbf{r}_x, \mathbf{r})_{[\mathcal{H}]^2} = \boldsymbol{\nu}(\mathbf{x}) \cdot \mathbf{r}(\mathbf{x}) \stackrel{(32)}{=} \boldsymbol{\nu}(\mathbf{x}) \cdot \mathbf{r}_N(\mathbf{x}) = (\mathbf{r}_x, \mathbf{r}_N)_{[\mathcal{H}]^2}.$$

Therefore,

$$(34) \quad (\mathbf{r}_x, \mathbf{r} - \mathbf{r}_N)_{[\mathcal{H}]^2} = 0 \quad \text{for all } \mathbf{x} \in \mathcal{X}_N. \quad \square$$

REMARK 2.19. *Lemma 2.18 implies that \mathbf{r}_N is the best approximation of \mathbf{r} in \mathcal{R}_N with respect to the $[\mathcal{H}]^2$ -norm, and that $\|\mathbf{r}_N\|_{[\mathcal{H}]^2} \leq \|\mathbf{r}\|_{[\mathcal{H}]^2}$.*

We conclude the section by showing that any function in $[\mathcal{H}(\partial\Omega)]^2$ can be approximated arbitrarily well using sufficiently many \mathbf{r}_x s.

THEOREM 2.20. *The set $\cup_{N \geq 1} \mathcal{R}_N$ is dense in $[\mathcal{H}(\partial\Omega)]_\nu^2$.*

Proof. Let $\{\mathcal{X}_N\}_{N \in \mathbb{N}}$ be a nested sequence of finite subsets (that contain pairwise distinct points) of $\partial\Omega$ such that the union $\cup_{N \in \mathbb{N}} \mathcal{X}_N$ is dense in $\partial\Omega$. For an arbitrary $\mathbf{r} \in [\mathcal{H}(\partial\Omega)]_\nu^2$, denote by \mathbf{r}_N its interpolant on \mathcal{R}_N (see [Lemma 2.18](#)).

The sequence $\{\mathbf{r}_N\}_{N \in \mathbb{N}}$ is bounded in $[\mathcal{H}(\partial\Omega)]^2$ because $\|\mathbf{r}_N\|_{[\mathcal{H}]^2} \leq \|\mathbf{r}\|_{[\mathcal{H}]^2}$ for every N . Therefore, there is a subsequence $\{\mathbf{r}_{N_i}\}_{i \in \mathbb{N}}$ that converges weakly to a function $\mathbf{f} \in [\mathcal{H}(\partial\Omega)]_\nu^2$. By Mazur's Lemma [6, p.61], there is a sequence $\{\hat{\mathbf{r}}_n\}_{n \in \mathbb{N}}$ of convex combinations of $\{\mathbf{r}_{N_i}\}_{i \in \mathbb{N}}$ that converges strongly in $[\mathcal{H}(\partial\Omega)]^2$ to \mathbf{f} . Note that there is a function $\mathcal{N} : \mathbb{N} \rightarrow \mathbb{N}$ such that $\mathcal{N}(n) \geq n$ and $\hat{\mathbf{r}}_n \in \mathcal{R}_{\mathcal{N}(n)}$ for every $n \in \mathbb{N}$.

We recall that in RKHS strong convergence implies pointwise convergence. Therefore, for every $\mathbf{z} \in \partial\Omega$,

$$(35) \quad \hat{\mathbf{r}}_n(\mathbf{z}) \rightarrow \mathbf{f}(\mathbf{z}) \quad \text{as } n \rightarrow \infty.$$

Additionally,

$$(36) \quad \hat{\mathbf{r}}_n(\mathbf{z}) = \mathbf{r}(\mathbf{z}) \quad \text{for every } \mathbf{z} \in \mathcal{X}_{\mathcal{N}(n)},$$

because $\hat{\mathbf{r}}_n$ is a convex combination of interpolants. Therefore, $\mathbf{f} = \mathbf{r}$ on $\cup_{n \in \mathbb{N}} \mathcal{X}_{\mathcal{N}(n)}$ and in turn, since $\cup_{n \in \mathbb{N}} \mathcal{X}_{\mathcal{N}(n)}$ is dense in $\partial\Omega$ and \mathbf{f} and \mathbf{r} are continuous, we conclude $\mathbf{f} = \mathbf{r}$ on $\partial\Omega$. It follows that $\hat{\mathbf{r}}_n$ converges strongly to \mathbf{r} . \square

2.4. Approximation of weakly-normal basis functions. The functions \mathbf{r}_x s introduced by [Definition 2.11](#) live in the infinite dimensional space $[\mathcal{H}(\partial\Omega)]^2$. In this section we explain how to approximate them using finitely many collocation points and analyse the numerical error of this approximation.

In this section, $\mathcal{X} = \{\mathbf{x}_1, \dots, \mathbf{x}_N\}$ and $\mathcal{Y} = \{\mathbf{y}_1, \dots, \mathbf{y}_M\}$, $M \leq N$, denote two subset of $\partial\Omega$ (containing pairwise distinct points) with $\mathcal{Y} \subset \mathcal{X}$. These sets are used to define the finite dimensional spaces

$$(37) \quad V_h(\mathcal{X}) = \text{span}\{\mathbf{k}(\mathbf{x}, \cdot)|_{\partial\Omega} : \mathbf{x} \in \mathcal{X}\} \quad \text{and} \quad V_h(\mathcal{Y}) = \text{span}\{\mathbf{k}(\mathbf{y}, \cdot)|_{\partial\Omega} : \mathbf{y} \in \mathcal{Y}\}.$$

Finally, we denote by $\mathcal{I}_{V_h} : \mathcal{H}(\partial\Omega) \rightarrow V_h(\mathcal{X})$ and $\mathcal{I}_{[V_h]^2} : [\mathcal{H}(\partial\Omega)]^2 \rightarrow [V_h(\mathcal{X})]^2$ the standard pointwise interpolation operators.

DEFINITION 2.21. *Let $\mathbf{x} \in \partial\Omega$. The finite dimensional approximation $(\mathbf{r}_\mathbf{x}^h, p_\mathbf{x}^h) \in [V_h(\mathcal{X})]^2 \times [V_h(\mathcal{Y})]$ of $(\mathbf{r}_\mathbf{x}, p_\mathbf{x})$ is characterised by*

$$(38a) \quad (\mathbf{r}_\mathbf{x}^h, \varphi)_{[\mathcal{H}]^2} + (\varphi \cdot \boldsymbol{\tau}, p_\mathbf{x}^h)_\mathcal{H} = \boldsymbol{\nu}(\mathbf{x}) \cdot \varphi(\mathbf{x}) \quad \text{for all } \varphi \in [V_h(\mathcal{X})]^2,$$

$$(38b) \quad (\mathbf{r}_\mathbf{x}^h \cdot \boldsymbol{\tau}, \psi)_\mathcal{H} = 0 \quad \text{for all } \psi \in V_h(\mathcal{Y}).$$

[Theorem 2.26](#) shows that [Definition 2.21](#) is well defined. Its proof relies on [Lemma 2.25](#), which is discrete counterpart of [Lemma 2.12](#). To prove this lemma, we use the following properties of the interpolation operators \mathcal{I}_{V_h} and $\mathcal{I}_{[V_h]^2}$.

LEMMA 2.22. *The interpolation operator \mathcal{I}_{V_h} is an \mathcal{H} -orthogonal projection.*

Proof. Let \mathbf{x} be a point from \mathcal{X} , and choose a $\psi \in \mathcal{H}[\partial\Omega]$. Since \mathbf{x} is an interpolation point, it holds that

$$(39) \quad (\mathcal{I}_{V_h}(\psi), \mathbf{k}(\mathbf{x}, \cdot))_{\mathcal{H}} = \mathcal{I}_{V_h}(\psi)(\mathbf{x}) = \psi(\mathbf{x}) = (\psi, \mathbf{k}(\mathbf{x}, \cdot))_{\mathcal{H}},$$

and thus,

$$(40) \quad (\mathcal{I}_{V_h}(\psi) - \psi, \phi)_{\mathcal{H}} = 0 \quad \text{for all } \phi \in V_h(\mathcal{X}). \quad \square$$

COROLLARY 2.23. *If Assumption 2.8 holds true, then the interpolation operator \mathcal{I}_{V_h} satisfies*

$$(41) \quad \|\mathcal{I}_{V_h}(f\psi)\|_{\mathcal{H}} \leq c_{\Omega} \|f\|_{C^k(\partial\Omega)} \|\psi\|_{\mathcal{H}}$$

for every $f \in C^k(\partial\Omega)$ and every $\psi \in \mathcal{H}(\partial\Omega)$.

Proof. Choose an $f \in C^k(\partial\Omega)$ and a $\psi \in \mathcal{H}(\partial\Omega)$. Since \mathcal{I}_{V_h} is an \mathcal{H} -orthogonal projection, $V_h(\mathcal{X}) \subset \mathcal{H}(\partial\Omega)$, and (9), it holds that

$$(42) \quad \|\mathcal{I}_{V_h}(f\psi)\|_{\mathcal{H}} \leq \|f\psi\|_{\mathcal{H}} \leq c_{\Omega} \|f\|_{C^k(\partial\Omega)} \|\psi\|_{\mathcal{H}}. \quad \square$$

COROLLARY 2.24. *If Assumption 2.8 holds true, then the interpolation operator $\mathcal{I}_{[V_h]^2}$ satisfies*

$$(43) \quad \|\mathcal{I}_{[V_h]^2}(\boldsymbol{\tau}\psi)\|_{[\mathcal{H}]^2} \leq c_{\Omega} \|\boldsymbol{\tau}\|_{C^k} \|\psi\|_{\mathcal{H}} \quad \text{for all } \psi \in \mathcal{H}(\partial\Omega).$$

Proof. Note that $\mathcal{I}_{[V_h]^2}(\boldsymbol{\tau}\psi) = \mathcal{I}_{V_h}(\boldsymbol{\tau} \cdot \mathbf{e}_1 \psi) \mathbf{e}_1 + \mathcal{I}_{V_h}(\boldsymbol{\tau} \cdot \mathbf{e}_2 \psi) \mathbf{e}_2$. Therefore, by Corollary 2.23,

$$\begin{aligned} \|\mathcal{I}_{[V_h]^2}(\boldsymbol{\tau}\psi)\|_{[\mathcal{H}]^2}^2 &= \|\mathcal{I}_{V_h}(\boldsymbol{\tau} \cdot \mathbf{e}_1 \psi)\|_{\mathcal{H}}^2 + \|\mathcal{I}_{V_h}(\boldsymbol{\tau} \cdot \mathbf{e}_2 \psi)\|_{\mathcal{H}}^2 \\ &\leq c_{\Omega}^2 \|\boldsymbol{\tau} \cdot \mathbf{e}_1\|_{C^k}^2 \|\psi\|_{\mathcal{H}}^2 + c_{\Omega}^2 \|\boldsymbol{\tau} \cdot \mathbf{e}_2\|_{C^k}^2 \|\psi\|_{\mathcal{H}}^2 \\ &= c_{\Omega}^2 \|\boldsymbol{\tau}\|_{C^k}^2 \|\psi\|_{\mathcal{H}}^2. \end{aligned} \quad \square$$

LEMMA 2.25 (discrete inf-sup condition). *The following holds*

$$(44) \quad \sup_{\substack{\boldsymbol{\varphi} \in [V_h(\mathcal{X})]^2, \\ \|\boldsymbol{\varphi}\|_{[\mathcal{H}]^2} \leq 1}} (\boldsymbol{\varphi} \cdot \boldsymbol{\tau}, \psi)_{\mathcal{H}} \geq \frac{\|\psi\|_{\mathcal{H}}}{c_{\Omega} \|\boldsymbol{\tau}\|_{C^k}} \quad \text{for all } \psi \in V_h(\mathcal{Y}).$$

Proof. Let $\psi \in V_h(\mathcal{Y})$. By Corollary 2.24,

$$(45) \quad \sup_{\substack{\boldsymbol{\varphi} \in [V_h(\mathcal{X})]^2, \\ \|\boldsymbol{\varphi}\|_{[\mathcal{H}]^2} \leq 1}} (\boldsymbol{\varphi} \cdot \boldsymbol{\tau}, \psi)_{\mathcal{H}} \geq \left(\boldsymbol{\tau} \cdot \frac{\mathcal{I}_{[V_h]^2}(\boldsymbol{\tau}\psi)}{\|\mathcal{I}_{[V_h]^2}(\boldsymbol{\tau}\psi)\|_{[\mathcal{H}]^2}}, \psi \right)_{\mathcal{H}} \geq \frac{(\boldsymbol{\tau} \cdot \mathcal{I}_{[V_h]^2}(\boldsymbol{\tau}\psi), \psi)_{\mathcal{H}}}{c_{\Omega} \|\boldsymbol{\tau}\|_{C^k} \|\psi\|_{\mathcal{H}}}.$$

Let $\mathbf{y} \in \mathcal{Y}$. Then, since $\mathcal{Y} \subset \mathcal{X}$,

$$\begin{aligned} (\boldsymbol{\tau} \cdot \mathcal{I}_{[V_h]^2}(\boldsymbol{\tau}\psi), \mathbf{k}(\mathbf{y}, \cdot))_{\mathcal{H}} &= \boldsymbol{\tau}(\mathbf{y}) \cdot \mathcal{I}_{[V_h]^2}(\boldsymbol{\tau}\psi)(\mathbf{y}) \\ &= \boldsymbol{\tau}(\mathbf{y}) \cdot (\boldsymbol{\tau}\psi)(\mathbf{y}) = \psi(\mathbf{y}) = (\psi, \mathbf{k}(\mathbf{y}, \cdot))_{\mathcal{H}}. \end{aligned}$$

Therefore, (44) follows by replacing $(\boldsymbol{\tau} \cdot \mathcal{I}_{[V_h]^2}(\boldsymbol{\tau}\psi), \psi)_{\mathcal{H}} = (\psi, \psi)_{\mathcal{H}} = \|\psi\|_{\mathcal{H}}^2$ into (45). \square

THEOREM 2.26. *The finite dimensional problem (38) has a unique solution, which satisfies*

$$(46) \quad \|\mathbf{r}_{\mathbf{x}}^h\|_{[\mathcal{H}]^2} \leq 1 \quad \text{and} \quad \|p_{\mathbf{x}}^h\|_{\mathcal{H}} \leq 2c_{\Omega}\|\boldsymbol{\tau}\|_{C^k}.$$

Moreover,

$$(47) \quad \|\mathbf{r}_{\mathbf{x}}^h - \mathbf{r}_{\mathbf{x}}\|_{[\mathcal{H}]^2} \leq \|\boldsymbol{\nu}\|_{C^k}^2 \inf_{\boldsymbol{\varphi} \in [V_h(\mathcal{X})]^2} \|\mathbf{r}_{\mathbf{x}} - \boldsymbol{\varphi}\|_{[\mathcal{H}]^2} + \|\boldsymbol{\tau}\|_{C^k} \inf_{\psi \in V_h(\mathcal{Y})} \|p_{\mathbf{x}} - \psi\|_{\mathcal{H}},$$

and

$$(48) \quad \|p_{\mathbf{x}}^h - p_{\mathbf{x}}\|_{\mathcal{H}} \leq c_{\Omega}\|\boldsymbol{\tau}\|_{C^k} \|\mathbf{r}_{\mathbf{x}}^h - \mathbf{r}_{\mathbf{x}}\|_{[\mathcal{H}]^2} + (1 + c_{\Omega}^2\|\boldsymbol{\tau}\|_{C^k}^2) \inf_{\psi \in V_h(\mathcal{Y})} \|p_{\mathbf{x}} - \psi\|_{\mathcal{H}}.$$

Proof. The functions $\mathbf{r}_{\mathbf{x}}^h$ and $p_{\mathbf{x}}^h$ can be written as

$$(49) \quad \mathbf{r}_{\mathbf{x}}^h = \sum_{i=1}^N \boldsymbol{\alpha}_i \mathbf{k}(\mathbf{x}_i, \cdot), \quad p_{\mathbf{x}}^h = \sum_{i=1}^M \beta_i \mathbf{k}(\mathbf{y}_j, \cdot),$$

where $\boldsymbol{\alpha}_i = (\alpha_i^1, \alpha_i^2)^\top \in \mathbf{R}^2$ and $\beta_i \in \mathbf{R}$ are certain unknown coefficients.

The vectors $\mathbf{a} := (\alpha_1^1, \dots, \alpha_N^1, \alpha_1^2, \dots, \alpha_N^2)^\top$ and $\mathbf{b} := (\beta_1, \dots, \beta_M)^\top$ satisfy

$$(50) \quad \begin{pmatrix} \mathbf{A} & \mathbf{B}^\top \\ \mathbf{B} & \mathbf{0} \end{pmatrix} \begin{pmatrix} \mathbf{a} \\ \mathbf{b} \end{pmatrix} = \begin{pmatrix} \mathbf{L} \\ \mathbf{0} \end{pmatrix},$$

where

$$(51) \quad \mathbf{A} = \begin{pmatrix} \tilde{\mathbf{A}} & \mathbf{0} \\ \mathbf{0} & \tilde{\mathbf{A}} \end{pmatrix}, \quad \mathbf{B} = (\mathbf{B}^1 \mathbf{B}^2), \quad \mathbf{L} = \begin{pmatrix} \mathbf{L}^1 \\ \mathbf{L}_2 \end{pmatrix},$$

and (with $\boldsymbol{\tau} = (\tau^1, \tau^2)^\top$ and $\boldsymbol{\nu} = (\nu^1, \nu^2)^\top$)

$$(52) \quad (\tilde{\mathbf{A}})_{n,m} = \mathbf{k}(\mathbf{x}_n, \mathbf{x}_m), \quad n, m = 1, \dots, N,$$

$$(53) \quad (\mathbf{B}^\ell)_{m,n} = \mathbf{k}(\mathbf{x}_n, \mathbf{y}_m) \tau^\ell(\mathbf{x}_n), \quad m = 1, \dots, M, \quad n = 1, \dots, N,$$

$$(54) \quad (\mathbf{L}^\ell)_n = \nu^\ell(\mathbf{x}) \mathbf{k}(\mathbf{x}_n, \mathbf{x}), \quad n = 1, \dots, N.$$

The linear system (50) has a unique solution because $\tilde{\mathbf{A}}$ (and thus \mathbf{A}) is positive-definite and \mathbf{B} has maximal rank M . The maximal rank of \mathbf{B} follows directly from Lemma 2.25. For a more direct proof, recall that $\mathcal{Y} \subset \mathcal{X}$. Therefore, the matrix \mathbf{B} contains the M column vectors $\{(\mathbf{k}(\mathbf{y}_i, \mathbf{y}_j) c_i)_{j=1, \dots, M} : i = 1, \dots, M\}$, where $c_i = \tau^1(\mathbf{y}_i)$ if $\tau^1(\mathbf{y}_i) \neq 0$ and $c_i = \tau^2(\mathbf{y}_i)$ otherwise (so that $c_i > 0$ for every i). These vectors are linearly independent because the kernel \mathbf{k} is positive-definite.

The estimate (46) follows by inserting $\boldsymbol{\varphi} = \mathbf{r}_{\mathbf{x}}^h$ into (38a) and using Cauchy-Schwarz and $\|\mathbf{k}(\mathbf{x}, \cdot)\|_{\mathcal{H}} = 1$ (see (20)). To prove the estimate on the multiplier $p_{\mathbf{x}}^h$, note that, by (44),

$$(55) \quad \|p_{\mathbf{x}}^h\| \leq c_{\Omega}\|\boldsymbol{\tau}\|_{C^k} \sup_{\substack{\boldsymbol{\varphi} \in [V_h(\mathcal{X})]^2, \\ \|\boldsymbol{\varphi}\|_{[\mathcal{H}]^2} \leq 1}} (\boldsymbol{\varphi} \cdot \boldsymbol{\tau}, p_{\mathbf{x}}^h)_{\mathcal{H}},$$

and that by (38a), for every $\boldsymbol{\varphi} \in [V_h(\mathcal{X})]^2$ with $\|\boldsymbol{\varphi}\|_{[\mathcal{H}]^2} \leq 1$,

$$\begin{aligned} (\boldsymbol{\varphi} \cdot \boldsymbol{\tau}, p_{\mathbf{x}}^h)_{\mathcal{H}} &= \boldsymbol{\nu}(\mathbf{x}) \cdot \boldsymbol{\varphi}(\mathbf{x}) - (\mathbf{r}_{\mathbf{x}}^h, \boldsymbol{\varphi})_{[\mathcal{H}]^2} \\ &\leq |\boldsymbol{\varphi}(\mathbf{x})| + \|\mathbf{r}_{\mathbf{x}}^h\|_{[\mathcal{H}]^2} \|\boldsymbol{\varphi}\|_{[\mathcal{H}]^2} \leq \|\boldsymbol{\varphi}\|_{[\mathcal{H}]^2} + 1 \leq 2. \end{aligned}$$

Finally, quasi-optimality results similar to (47) and (48) can be derived by applying directly [2, Prop. 5.2.1, pp 274]. Here, we give explicit details on the derivation of (47) and (48).

To show (47), note that the differences $\mathbf{r}_x^h - \mathbf{r}_x$ and $p_x^h - p_x$ satisfy

$$(56a) \quad (\mathbf{r}_x^h - \mathbf{r}_x, \varphi)_{[\mathcal{H}]^2} + (\varphi \cdot \boldsymbol{\tau}, p_x^h - p_x)_{\mathcal{H}} = 0 \quad \text{for all } \varphi \in [V_h(\mathcal{X})]^2,$$

$$(56b) \quad ((\mathbf{r}_x^h - \mathbf{r}_x) \cdot \boldsymbol{\tau}, \psi)_{\mathcal{H}} = 0 \quad \text{for all } \psi \in V_h(\mathcal{Y}).$$

This implies that

$$\begin{aligned} \|\mathbf{r}_x^h - \mathbf{r}_x\|_{[\mathcal{H}]^2}^2 &= (\mathbf{r}_x^h - \mathbf{r}_x, \mathbf{r}_x^h - \mathbf{r}_x)_{[\mathcal{H}]^2} \\ &= (\mathbf{r}_x^h - \mathbf{r}_x, \mathbf{r}_x^h)_{[\mathcal{H}]^2} - (\mathbf{r}_x^h - \mathbf{r}_x, \mathbf{r}_x)_{[\mathcal{H}]^2} \\ &= -(\mathbf{r}_x^h \cdot \boldsymbol{\tau}, p_x^h - p_x)_{\mathcal{H}} - (\mathbf{r}_x^h - \mathbf{r}_x, \mathbf{r}_x)_{[\mathcal{H}]^2} \\ &= -(\mathbf{r}_x^h \cdot \boldsymbol{\tau}, p_x^h)_{\mathcal{H}} + (\mathbf{r}_x^h \cdot \boldsymbol{\tau}, p_x)_{\mathcal{H}} - (\mathbf{r}_x^h - \mathbf{r}_x, \mathbf{r}_x)_{[\mathcal{H}]^2} \\ &= (\mathbf{r}_x^h \cdot \boldsymbol{\tau}, p_x)_{\mathcal{H}} - (\mathbf{r}_x^h - \mathbf{r}_x, \mathbf{r}_x)_{[\mathcal{H}]^2} \\ &= (\mathbf{r}_x^h \cdot \boldsymbol{\tau}, p_x)_{\mathcal{H}} - (\mathbf{r}_x^h - \mathbf{r}_x, (\mathbf{r}_x \cdot \boldsymbol{\nu}) \cdot \boldsymbol{\nu})_{[\mathcal{H}]^2}. \end{aligned}$$

The latter result combined with (56) implies that, for any $\varphi \in [V_h(\mathcal{X})]^2$ and any $\psi \in V_h(\mathcal{Y})$,

$$(57) \quad \|\mathbf{r}_x^h - \mathbf{r}_x\|_{[\mathcal{H}]^2}^2 = (\mathbf{r}_x^h \cdot \boldsymbol{\tau} - \mathbf{r}_x \cdot \boldsymbol{\tau}, p_x - \psi)_{\mathcal{H}} - (\mathbf{r}_x^h - \mathbf{r}_x, (\mathbf{r}_x \cdot \boldsymbol{\nu}) \cdot \boldsymbol{\nu} - (\varphi \cdot \boldsymbol{\nu}) \boldsymbol{\nu})_{[\mathcal{H}]^2}.$$

Then, Cauchy-Schwarz inequality and (9) imply

$$\begin{aligned} \|\mathbf{r}_x^h - \mathbf{r}_x\|_{[\mathcal{H}]^2}^2 &\leq \|\mathbf{r}_x^h \cdot \boldsymbol{\tau} - \mathbf{r}_x \cdot \boldsymbol{\tau}\|_{\mathcal{H}} \|p_x - \psi\|_{\mathcal{H}} + \|\mathbf{r}_x^h - \mathbf{r}_x\|_{[\mathcal{H}]^2} \|((\mathbf{r}_x - \varphi) \cdot \boldsymbol{\nu}) \boldsymbol{\nu}\|_{[\mathcal{H}]^2}, \\ (58) \quad &\leq \|\mathbf{r}_x^h - \mathbf{r}_x\|_{[\mathcal{H}]^2} (\|\boldsymbol{\tau}\|_{C^k} \|p_x - \psi\|_{\mathcal{H}} + \|\boldsymbol{\nu}\|_{C^k}^2 \|\mathbf{r}_x - \varphi\|_{[\mathcal{H}]^2}), \end{aligned}$$

from which (47) follows easily.

To show (48), note that for any $\psi \in V_h(\mathcal{Y})$, (44) implies

$$(59) \quad \|p_x^h - \psi\|_{\mathcal{H}} \leq c_{\Omega} \|\boldsymbol{\tau}\|_{C^k} \sup_{\substack{\varphi \in [V_h(\mathcal{X})]^2, \\ \|\varphi\|_{[\mathcal{H}]^2} \leq 1}} (\varphi \cdot \boldsymbol{\tau}, p_x^h - \psi)_{\mathcal{H}}.$$

For any $\varphi \in [V_h(\mathcal{X})]^2$, (10) and (38) imply

$$\begin{aligned} (\varphi \cdot \boldsymbol{\tau}, p_x^h - \psi)_{\mathcal{H}} &= (\varphi \cdot \boldsymbol{\tau}, p_x^h)_{\mathcal{H}} - (\varphi \cdot \boldsymbol{\tau}, \psi)_{\mathcal{H}} \\ &= \boldsymbol{\nu}(\mathbf{x}) \cdot \varphi(\mathbf{x}) - (\mathbf{r}_x^h, \varphi)_{[\mathcal{H}]^2} - (\varphi \cdot \boldsymbol{\tau}, \psi)_{\mathcal{H}} \\ &= (\mathbf{r}_x, \varphi)_{[\mathcal{H}]^2} + (\varphi \cdot \boldsymbol{\tau}, p_x)_{\mathcal{H}} - (\mathbf{r}_x^h, \varphi)_{[\mathcal{H}]^2} - (\varphi \cdot \boldsymbol{\tau}, \psi)_{\mathcal{H}} \\ &= (\mathbf{r}_x - \mathbf{r}_x^h, \varphi)_{[\mathcal{H}]^2} + (\varphi \cdot \boldsymbol{\tau}, p_x - \psi)_{\mathcal{H}} \\ &\leq \|\boldsymbol{\psi}\|_{[\mathcal{H}]^2} (\|\mathbf{r}_x - \mathbf{r}_x^h\|_{[\mathcal{H}]^2} + c_{\Omega} \|\boldsymbol{\tau}\|_{C^k} \|p_x - \psi\|_{\mathcal{H}}), \end{aligned}$$

where the last inequality follows from Cauchy-Schwarz inequality and (9). Therefore,

$$(60) \quad \|p_x^h - \psi\|_{\mathcal{H}} \leq c_{\Omega} \|\boldsymbol{\tau}\|_{C^k} (\|\mathbf{r}_x - \mathbf{r}_x^h\|_{[\mathcal{H}]^2} + c_{\Omega} \|\boldsymbol{\tau}\|_{C^k} \|p_x - \psi\|_{\mathcal{H}}),$$

and, by the triangle inequality,

$$\begin{aligned} \|p_x - p_x^h\|_{\mathcal{H}} &\leq \|p_x - \psi\|_{\mathcal{H}} + \|p_x^h - \psi\|_{\mathcal{H}} \\ &\leq c_{\Omega} \|\boldsymbol{\tau}\|_{C^k} \|\mathbf{r}_x - \mathbf{r}_x^h\|_{[\mathcal{H}]^2} + (1 + c_{\Omega}^2 \|\boldsymbol{\tau}\|_{C^k}^2) \|p_x - \psi\|_{\mathcal{H}}. \end{aligned} \quad \square$$

The following corollary follows directly from the quasi-optimality estimates (47) and (48)

COROLLARY 2.27. *Let $\{\mathcal{Y}_N\}_{N \in \mathbb{N}}$ be a nested sequence of finite subsets (that contain pairwise distinct points) of $\partial\Omega$ such that the union $\cup_{N \in \mathbb{N}} \mathcal{Y}_N$ is dense in $\partial\Omega$. Then, the sequence of functions $(\mathbf{r}_\mathbf{x}^{h_N}, p_\mathbf{x}^{h_N})$ converges strongly to $(\mathbf{r}_\mathbf{x}, p_\mathbf{x})$.*

Before studying convergence rates, we mention that in [22] Sturm proved superlinear convergence of a shape Newton method in the Micheletti space based on functions of the form $\mathbf{k}(\mathbf{x}, \cdot)\boldsymbol{\nu}(\mathbf{x})$. The next lemma shows that such functions arise from a particular discretisation of (10).

PROPOSITION 2.28. *If $M = 1$ and $\mathcal{Y} = \{\mathbf{x}\} \subset \mathcal{X}$, then the solution of (38) is*

$$\mathbf{r}_\mathbf{x}^h(\cdot) = \mathbf{k}(\mathbf{x}, \cdot)\boldsymbol{\nu}(\mathbf{x}), \quad p_\mathbf{x}^h = 0.$$

Proof. By Theorem 2.26, we only need to verify that the pair $(\mathbf{r}_\mathbf{x}^h, p_\mathbf{x}^h)$ satisfies (38). By the reproducing kernel property,

$$(\mathbf{r}_\mathbf{x}^h, \boldsymbol{\varphi})_{[\mathcal{H}]^2} = \boldsymbol{\nu}(\mathbf{x}) \cdot \boldsymbol{\varphi}(\mathbf{x}) \quad \text{for all } \boldsymbol{\varphi} \in [\mathcal{H}(\partial\Omega)]^2,$$

which, together with $p_\mathbf{x}^h = 0$, implies (38a). Finally,

$$(61) \quad (\mathbf{r}_\mathbf{x}^h \cdot \boldsymbol{\tau}, k(\mathbf{x}, \cdot))_{\mathcal{H}} = \mathbf{k}(\mathbf{x}, \mathbf{x})\boldsymbol{\tau}(\mathbf{x}) \cdot \boldsymbol{\nu}(\mathbf{x}) = 0,$$

together with $V_h(\mathcal{Y}) = \text{span}\{\mathbf{k}(\mathbf{x}, \cdot)\}$, implies (38b). \square

Henceforth, we restrict ourselves to radial kernels, for which a solid interpolation theory on submanifolds is available.

ASSUMPTION 2.29. *The kernel \mathbf{k} satisfies $\mathbf{k}(\mathbf{x}, \mathbf{y}) = \Phi(\mathbf{x} - \mathbf{y})$ for a positive definite function $\Phi \in L_2(\mathbf{R}^d) \cap C(\mathbf{R}^d)$. Assume that the Fourier transform $\hat{\Phi}$ of Φ satisfies*

$$(62) \quad c_1(1 + \|\mathbf{x}\|^2)^{-\xi} \leq \hat{\Phi}(\mathbf{x}) \leq c_2(1 + \|\mathbf{x}\|^2)^{-\xi} \quad \text{for all } \mathbf{x} \in \mathbf{R}^2,$$

with $\xi > 1$ and two constants $c_1, c_2 > 0$, $c_1 \leq c_2$.

REMARK 2.30. *Assumption 2.29 implies that the native space of \mathbf{k} on \mathbf{R}^2 is $\mathcal{H}(\mathbf{R}^2) = H^\xi(\mathbf{R}^2)$ with equivalent norms. Thus, by the Sobolev trace theorem, the native space of \mathbf{k} on $\partial\Omega$ is $\mathcal{H}(\partial\Omega) = H^{\xi-1/2}(\partial\Omega)$ [10, Prop. 5].*

For such kernels, we can derive convergence rates of $\mathbf{r}_\mathbf{x}^h$ to $\mathbf{r}_\mathbf{x}$ and $p_\mathbf{x}^h$ to $p_\mathbf{x}$ in certain Sobolev spaces. For shortness, we focus on the more interesting term $\mathbf{r}_\mathbf{x}$ (convergence rates of $p_\mathbf{x}^h$ can be derived in exactly the same way). Before stating the theorem, we recall the concept of fill distance of discrete sets.

DEFINITION 2.31. *The fill distance associated with a set $\mathcal{X} \subset \partial\Omega$ is defined by*

$$(63) \quad h_{\mathcal{X}, \partial\Omega} := \sup_{\mathbf{y} \in \partial\Omega} \inf_{\mathbf{x} \in \mathcal{X}} d_{\partial\Omega}(\mathbf{x}, \mathbf{y}),$$

where $d_{\partial\Omega}$ denotes the geodesic distance associated with $\partial\Omega$. Note that $d_{\partial\Omega}$ is equivalent to the Euclidean metric restricted on $\partial\Omega$ [10, Theorem 6], that is, there are two constants $c_1, c_2 > 0$ (that depend only on $\partial\Omega$) such that

$$(64) \quad c_1\|\mathbf{x} - \mathbf{y}\| \leq d_{\partial\Omega}(\mathbf{x}, \mathbf{y}) \leq c_2\|\mathbf{x} - \mathbf{y}\| \quad \text{for all } \mathbf{x}, \mathbf{y} \in \partial\Omega.$$

Given a continuous kernel k we define the integral operator $T : L_2(\partial\Omega) \rightarrow L_2(\partial\Omega)$ via

$$(65) \quad f \mapsto \left(Tf : \mathbf{x} \mapsto \int_{\partial\Omega} k(\mathbf{x}, \mathbf{s}) f(\mathbf{s}) \, d\mathbf{s} \right).$$

We define similarly the integral operator \mathbf{T} that acts on $L_2(\partial\Omega, \mathbf{R}^2)$.

THEOREM 2.32. *Let $\mathcal{Y} = \mathcal{X}$ and $\xi > 1$, and $s = \xi - 1/2$. Let k be satisfying Assumption 2.29, so that $\mathcal{H}(\partial\Omega) := H^s(\partial\Omega)$. Assume that $T^{-1}(p_{\mathbf{x}}) \in L_2(\partial\Omega)$ and $\mathbf{T}^{-1}(\mathbf{r}_{\mathbf{x}}) \in L_2(\partial\Omega, \mathbf{R}^2)$. Then, there is a constant $c_{\partial\Omega} > 0$, such that*

$$(66) \quad \|\mathbf{r}_{\mathbf{x}}^{h_{\mathcal{X}}, \partial\Omega} - \mathbf{r}_{\mathbf{x}}\|_{H^s(\partial\Omega)} \leq c_{\partial\Omega} h_{\mathcal{X}, \partial\Omega}^s (\|\boldsymbol{\nu}\|_{C^k}^2 \|\mathbf{T}^{-1} \mathbf{r}_{\mathbf{x}}\|_{L_2(\partial\Omega, \mathbf{R}^2)} + \|\boldsymbol{\tau}\|_{C^k} \|T^{-1} p_{\mathbf{x}}\|_{L_2(\partial\Omega)})$$

for all $h_{\mathcal{X}, \partial\Omega} \leq h_{\partial\Omega}$.

Proof. In Corollary 15 from [10] it is shown that there is a constant $c > 0$, such that

$$(67) \quad \|\mathcal{I}_{V_h}(\psi) - \psi\|_{\mathcal{H}} \leq c h_{\mathcal{X}, \partial\Omega}^s \|T^{-1} \psi\|_{L_2(\partial\Omega)} \quad \text{for all } \psi \in \mathcal{H}(\partial\Omega).$$

A similar result holds for the operator \mathbf{T} . Hence replacing $\boldsymbol{\varphi} = \mathcal{I}_{[V_h]^2}(\mathbf{r}_{\mathbf{x}})$ and $\psi = \mathcal{I}_{V_h}(p_{\mathbf{x}})$ in (47) andd using estimate (67) gives the desired results. \square

COROLLARY 2.33. *Let the hypotheses of Theorem 2.32 be satisfied. Then, there is a constant c such that*

$$(68) \quad \|\mathbf{r}_{\mathbf{x}}^{h_{\mathcal{X}}, \partial\Omega} - \mathbf{r}_{\mathbf{x}}\|_{L_2(\partial\Omega, \mathbf{R}^2)} \leq c h_{\mathcal{X}, \partial\Omega}^{2s}$$

for all $h_{\mathcal{X}, \partial\Omega} \leq h_{\partial\Omega}$.

Proof. Applying [10, Lem. 10] yields

$$(69) \quad \|\boldsymbol{\varphi} - \mathcal{I}_{[V_h]^2}(\boldsymbol{\varphi})\|_{L_2(\partial\Omega, \mathbf{R}^2)} \leq c h_{\mathcal{X}, \partial\Omega}^s \|\boldsymbol{\varphi} - \mathcal{I}_{[V_h]^2}(\boldsymbol{\varphi})\|_{\mathcal{H}}$$

for all $\boldsymbol{\varphi} \in [\mathcal{H}(\partial\Omega)]^2$ (and similarly for \mathcal{I}_{V_h}). Hence combining this inequality with (66) gives the desired estimate. \square

NUMERICAL EXPERIMENT 2.34. *We perform a numerical experiment to verify the convergence rates derived in Theorem 2.32. We choose $\partial\Omega$ to be the ellipse depicted in Figure 1 (left) and consider the sequence of subsets*

$$(70) \quad \mathcal{X}_N = \{\gamma(2\pi\ell/N) : \ell = 1, \dots, N\} \quad \text{with} \quad N = 2^4, 2^5, \dots, 2^{10},$$

Then, for each N , we compute $\mathbf{r}_{\gamma(0)}^{h_N}$, where h_N denotes the fill distance of \mathcal{X}_N . Finally, we compute (with sufficiently many quadrature points) the $L_2(\partial\Omega)$ -absolute error using $\mathbf{r}_{\gamma(0)}^{h_{2^{10}}}$ as reference solution. In Figure 2, we plot these L_2 -errors versus h_N (measured with the Euclidean distance) for the kernels $k_4^{1,2}$, $k_6^{1,2}$, and $k_8^{1,2}$. The measured convergence rates read (approximatively) 4.51, 6.79, and 8.77, respectively, and are slightly better but still in line with Corollary 2.33. Similar comparable results are obtained for the nonconvex domain depicted in Figure 1 (left), as well as for different values of σ .

REMARK 2.35. *It is known from scattered data approximation theory [16] that the condition number of $(k(\mathbf{x}_i, \mathbf{x}_j))_{i,j=1}^n$ can be very large for certain collections of points $\{\mathbf{x}_i\}_{i=1}^n$. We have computed the condition number of the saddle point matrix from (50) for different σ s and h_N and have observed that, similarly to the condition number of $(k(\mathbf{x}_i, \mathbf{x}_j))_{i,j=1}^n$, it behaves roughly as $(\sigma/h_N)^p$, where p is the polynomial order of the Wendland's kernel.*

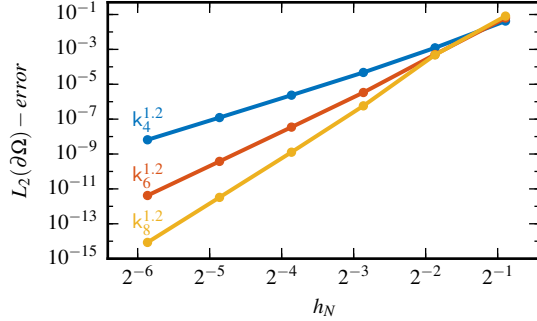


FIG. 2. *Numerical Experiment 2.34* confirms the convergence rates predicted by *Corollary 2.33*: the error $\|\mathbf{r}_x^{h_N} - \mathbf{r}_x\|_{L_2(\partial\Omega)}$ decays with the algebraic rate 4.51 (for $k_4^{1,2}$), 6.79 (for $k_6^{1,2}$), and 8.77 (for $k_8^{1,2}$).

3. Application to shape Newton methods. In this section, we briefly recall the shape Newton method introduced in [22], discuss its discretisation with the weakly-normal functions \mathbf{r}_x s, and perform some numerical simulations for an unconstrained shape optimisation test case. This test case is kept simple on purpose in order to restrict the discretization error to the use of weakly-normal basis functions. In this section, we use $\mathcal{X} = \mathcal{Y}$ in *Definition 2.21*.

3.1. Shape derivatives and their structure theorem. We begin by recalling the definition of shape derivatives and their structure theorem from [22]. For a given set $D \subset \mathbf{R}^2$, we denote by $\wp(D)$ the powerset of D .

DEFINITION 3.1. *Let $J : \Xi \subset \wp(D) \rightarrow \mathbf{R}$ be a shape function, and let $\mathbf{X}, \mathbf{Y} \in \mathring{C}^1(\bar{D}, \mathbf{R}^2)$ be two vector fields.*

(i) *The directional derivative of J at $\Omega \in \Xi$ in the direction \mathbf{X} is defined by*

$$(71) \quad DJ(\Omega)(\mathbf{X}) := \lim_{t \rightarrow 0^+} \frac{J((\mathbf{id} + t\mathbf{X})(\Omega)) - J(\Omega)}{t}.$$

(ii) *The second directional derivative of J at Ω in the direction (\mathbf{X}, \mathbf{Y}) is defined by*

$$(72) \quad \mathfrak{D}^2 J(\Omega)(\mathbf{X})(\mathbf{Y}) = \lim_{t \rightarrow 0^+} \frac{DJ((\mathbf{id} + t\mathbf{Y})(\Omega))(\mathbf{X} \circ (\mathbf{id} + t\mathbf{Y})^{-1}) - DJ(\Omega)(\mathbf{X})}{t},$$

(assuming that $DJ((\mathbf{id} + t\mathbf{Y})(\Omega))(\mathbf{X} \circ (\mathbf{id} + t\mathbf{Y})^{-1})$ exists for all small t).

We denote by $\nabla^\tau f$ the tangential gradient of function f and by $\mathbf{X}_\tau := \mathbf{X}|_{\partial\Omega} - (\mathbf{X}|_{\partial\Omega} \cdot \boldsymbol{\nu})\boldsymbol{\nu}$ the tangential component of a vector field \mathbf{X} on $\partial\Omega$. The shape derivatives DJ and $\mathfrak{D}^2 J$ are characterised by the following structure theorem (see [14, 22]).

THEOREM 3.2. *Assume that J is twice differentiable at Ω and assume that Ω is of class C^3 . Then, there are continuous functionals $\mathfrak{g} : C^1(\partial\Omega) \rightarrow \mathbf{R}$ and $\mathfrak{l} : C^1(\partial\Omega) \times C^1(\partial\Omega) \rightarrow \mathbf{R}$, such that*

$$(73) \quad DJ(\Omega)(\mathbf{X}) = \mathfrak{g}(\mathbf{X}|_{\partial\Omega} \cdot \boldsymbol{\nu}) \quad \text{for all } \mathbf{X} \in \mathring{C}^1(\bar{D}, \mathbf{R}^2),$$

and

$$(74) \quad \begin{aligned} \mathfrak{D}^2 J(\Omega)(\mathbf{X})(\mathbf{Y}) = & \mathfrak{l}(\mathbf{X}|_{\partial\Omega} \cdot \boldsymbol{\nu}, \mathbf{Y}|_{\partial\Omega} \cdot \boldsymbol{\nu}) - \mathfrak{g}(\partial^\tau \mathbf{X}_\tau \mathbf{Y}_\tau \cdot \boldsymbol{\nu}) \\ & - \mathfrak{g}(\nabla^\tau(\mathbf{Y} \cdot \boldsymbol{\nu}) \cdot \mathbf{X}_\tau) - \mathfrak{g}(\nabla^\tau(\mathbf{X} \cdot \boldsymbol{\nu}) \cdot \mathbf{Y}_\tau) \end{aligned}$$

for all $\mathbf{X}, \mathbf{Y} \in \mathring{C}^2(\bar{\Omega}, \mathbf{R}^2)$.

REMARK 3.3. Notice that (74) is equivalent to (see [14])

$$(75) \quad \mathfrak{D}^2 J(\Omega)(\mathbf{X})(\mathbf{Y}) = \mathfrak{l}(\mathbf{X}|_{\partial\Omega} \cdot \boldsymbol{\nu}, \mathbf{Y}|_{\partial\Omega} \cdot \boldsymbol{\nu}) - \mathfrak{g}(\boldsymbol{\nu} \cdot \partial^\tau \mathbf{Y} \mathbf{X}_\tau) - \mathfrak{g}(\mathbf{Y}_\tau \cdot \partial^\tau \boldsymbol{\nu} \mathbf{X}_\tau) - \mathfrak{g}(\boldsymbol{\nu} \cdot \partial^\tau X \mathbf{Y}_\tau).$$

3.2. Shape Newton descent directions and their approximation. In this section, we define the shape Newton equation and its approximation with weakly-normal basis functions. For a particular test case, we derive quasi-optimality of the approximate Newton update and verify the resulting convergence rates with a numerical experiment. Henceforth, $\Omega \subset \mathbf{R}^2$ is a set with C^{k+1} -boundary (with $k \geq 1$), and $\mathcal{H}(\mathbf{R}^2)$ is a RKHS that satisfies [Assumption 2.8](#).

DEFINITION 3.4. The $\mathcal{H}(\mathbf{R}^2)$ -Newton descent direction at Ω is the solution $\mathbf{X}_\boldsymbol{\nu} \in [\mathcal{H}(\partial\Omega)]_\boldsymbol{\nu}$ of

$$(76) \quad \mathfrak{D}^2 J(\Omega)(\mathbf{X}_\boldsymbol{\nu})(\mathbf{Y}) = -D J(\Omega)(\mathbf{Y}) \quad \text{for all } \mathbf{Y} \in [\mathcal{H}(\partial\Omega)]_\boldsymbol{\nu}^2.$$

REMARK 3.5. If $\mathcal{H}(\partial\Omega) \subset C^2(\partial\Omega)$ and J satisfies the assumptions of [Theorem 3.2](#), then

$$(77) \quad \mathfrak{D}^2 J(\Omega)(\mathbf{r}_x)(\mathbf{r}_y) = \mathfrak{l}(\mathbf{r}_x \cdot \boldsymbol{\nu}, \mathbf{r}_y \cdot \boldsymbol{\nu}) \quad \text{and} \quad D J(\Omega)(\mathbf{r}_y) = \mathfrak{g}(\mathbf{r}_y \cdot \boldsymbol{\nu}) \quad \text{for all } x, y \in \partial\Omega.$$

This, in light of [Theorem 2.20](#), implies that (76) is equivalent to

$$(78) \quad \mathfrak{l}(\mathbf{X}_\boldsymbol{\nu} \cdot \boldsymbol{\nu}, \mathbf{r}_y \cdot \boldsymbol{\nu}) = -\mathfrak{g}(\mathbf{r}_y \cdot \boldsymbol{\nu}) \quad \text{for all } y \in \partial\Omega.$$

Since \mathfrak{l} and \mathfrak{g} are (bi)linear and continuous in $C^1(\mathbf{R}^2)$, equation (78) can also be used to define $\mathcal{H}(\mathbf{R}^2)$ -Newton descent direction for RKHS that satisfy only $\mathcal{H}(\mathbf{R}^2) \subset C^1(\mathbf{R}^2)$. For instance, as mentioned before, the kernel \mathfrak{k}_2^g has the native space $\mathcal{H}(\mathbf{R}^2) = H^{2.5}(\mathbf{R}^2)$ and by the Sobolev inequality we have $H^{2.5}(\mathbf{R}^2) \subset C^{1,1/2}(\mathbf{R}^2)$, (where $C^{1,1/2}(\mathbf{R}^2)$ denotes the usual Hölder space).

In general, it can be difficult to compute an explicit solution of (76) because $\mathfrak{D}^2 J$ and $D J$ are typically given by very complicated formulas. For instance, when J is constrained by a PDE, the formula of $\mathfrak{D}^2 J$ contains the material derivative of the solution of the PDE-constraint [3]. Nevertheless, approximate $\mathcal{H}(\mathbf{R}^2)$ -Newton descent directions can be computed by discretising (76) with the weakly-normal basis functions \mathbf{r}_x s.

DEFINITION 3.6. Let $\mathcal{X}_N = \{\mathbf{x}_1, \dots, \mathbf{x}_N\} \subset \partial\Omega$ be a collection of pairwise distinct points, and let $h = h_{\mathcal{X}_N, \partial\Omega}$ denote its fill distance. The approximate $\mathcal{H}(\mathbf{R}^2)$ -Newton descent direction at Ω with respect to $\mathcal{H}(\partial\Omega)$ is the solution $\mathbf{X}_\boldsymbol{\nu}^h \in \mathcal{R}_N := \text{span}\{\mathbf{r}_x : x \in \mathcal{X}_N\}$, of

$$(79) \quad \mathfrak{D}^2 J(\Omega)(\mathbf{X}_\boldsymbol{\nu}^h)(\mathbf{Y}) = -D J(\Omega)(\mathbf{Y}) \quad \text{for all } \mathbf{Y} \in \mathcal{R}_N.$$

EXAMPLE 3.7. We consider the shape function $J(\Omega) = \int_\Omega f \, dx$ with $f \in C^2(\mathbf{R}^2)$. This shape function J can be used as a regularisation in image segmentation; see [12]. Its shape derivatives read [22]

$$(80) \quad D J(\Omega)(\mathbf{X}) = \int_{\partial\Omega} f \mathbf{X} \cdot \boldsymbol{\nu} \, ds,$$

$$(81) \quad \mathfrak{D}^2 J(\Omega)(\mathbf{X})(\mathbf{Y}) = \int_{\partial\Omega} (\nabla f \cdot \boldsymbol{\nu} + \kappa f)(\mathbf{X} \cdot \boldsymbol{\nu})(\mathbf{Y} \cdot \boldsymbol{\nu}) \, ds - \int_{\partial\Omega} f \boldsymbol{\nu} \cdot \partial^\tau \mathbf{X}_\tau \mathbf{Y}_\tau \, ds \\ - \int_{\partial\Omega} f \nabla^\tau (\mathbf{Y} \cdot \boldsymbol{\nu}) \cdot \mathbf{X} + f \nabla^\tau (\mathbf{X} \cdot \boldsymbol{\nu}) \cdot \mathbf{Y} \, ds,$$

where κ denotes the curvature of $\partial\Omega$. Hence the $\mathcal{H}(\mathbf{R}^2)$ -Newton descent direction at Ω is the solution $\mathbf{X}_\nu \in [\mathcal{H}(\partial\Omega)]_\nu$ of

$$(82) \quad \int_{\partial\Omega} (\nabla f \cdot \nu + \kappa f)(X_\nu \cdot \nu)(Y \cdot \nu) \, ds = - \int_{\partial\Omega} f(Y \cdot \nu) \, ds \quad \text{for all } Y \in [\mathcal{H}(\partial\Omega)]_\nu.$$

Note the when it exists, the solution of (82) is $\mathbf{X}_\nu = (-f/(\nabla f \cdot \nu + \kappa f))\nu$. Clearly, it is possible to approximate \mathbf{X}_ν by interpolating it on \mathcal{R}_N . However, note that such an interpolant would not satisfy (79).

Proposition 3.8 shows quasi-optimality of the approximate shape Newton updates when the shape derivatives are as in [Example 3.7](#).

PROPOSITION 3.8. *Let $J(\Omega) = \int_\Omega f \, dx$ with $f \in C^2(\mathbf{R}^2)$, and further assume that $\nabla f \cdot \nu + \kappa f > 0$ on $\partial\Omega$. Then, the solution $\mathbf{X}_\nu^h \in \mathcal{R}_N$ of (79) satisfies*

$$(83) \quad \|\mathbf{X}_\nu - \mathbf{X}_\nu^h\|_{L_2(\partial\Omega)} \leq c_{f,\Omega} \inf_{\mathbf{Y} \in \mathcal{R}_N} \|\mathbf{X}_\nu - \mathbf{Y}\|_{L_2(\partial\Omega)}.$$

Proof. The bilinear form

$$(84) \quad L_2(\partial\Omega) \times L_2(\partial\Omega) \rightarrow \mathbb{R}, \quad (x, y) \mapsto \int_{\partial\Omega} (\nabla f \cdot \nu + \kappa f) xy \, ds$$

is $L_2(\partial\Omega)$ -continuous, symmetric, and $L_2(\partial\Omega)$ -elliptic. Let $\mathcal{Z}_N := \{\mathbf{X} \cdot \nu : \mathbf{X} \in \mathcal{R}_N\}$. Clearly, $\mathcal{Z}_N \subset L_2(\partial\Omega)$. Therefore, the solution $z_h \in \mathcal{Z}_N$ of

$$(85) \quad \int_{\partial\Omega} (\nabla f \cdot \nu + \kappa f) z_h y \, ds = - \int_{\partial\Omega} f y \, ds \quad \text{for all } y \in \mathcal{Z}_N$$

satisfies

$$(86) \quad \|z - z_h\|_{L_2(\partial\Omega)} \leq c_{f,\Omega} \inf_{y \in \mathcal{Z}_N} \|z - y\|_{L_2(\partial\Omega)},$$

where $z \in L_2(\partial\Omega)$ is the solution of

$$(87) \quad \int_{\partial\Omega} (\nabla f \cdot \nu + \kappa f) z y \, ds = - \int_{\partial\Omega} f y \, ds \quad \text{for all } y \in L_2(\partial\Omega).$$

Finally, $\mathbf{X}_\nu^h = z_h \nu$, because \mathcal{R}_N satisfies $\mathcal{R}_N = \{z \nu : z \in \mathcal{Z}_N\}$, and $\mathbf{X}_\nu = z \nu$, because the solution of (87) is $z = -f/(\nabla f \cdot \nu + \kappa f)$. \square

NUMERICAL EXPERIMENT 3.9. *We perform a numerical experiment to investigate the approximation error (83) for $f(\mathbf{x}) = |\mathbf{x}|^2 - 1$. We choose $\partial\Omega$ to be the ellipse depicted in [Figure 1](#) (left) and consider the sequence of subsets*

$$(88) \quad \mathcal{X}_N = \{\gamma(2\pi\ell/N) : \ell = 1, \dots, N\} \quad \text{with} \quad N = 2^4, 2^5, \dots, 2^8,$$

For each N , we construct the finite dimensional space $\tilde{\mathcal{R}}_N := \{\mathbf{r}_\mathbf{x}^{h_N} : \mathbf{x} \in \mathcal{X}_N\}$ (where h_N denotes the fill distance of \mathcal{X}_N), and compute the solution $\tilde{\mathbf{X}}_\nu^{h_N} \in \tilde{\mathcal{R}}_N$ of

$$(89) \quad \int_{\partial\Omega} (\nabla f \cdot \nu + \kappa f)(\tilde{\mathbf{X}}_\nu^{h_N} \cdot \nu)(Y \cdot \nu) \, ds = - \int_{\partial\Omega} f(Y \cdot \nu) \, ds \quad \text{for all } Y \in \tilde{\mathcal{V}}_{h_N}.$$

Finally, we compute (with sufficiently many quadrature points) the $L_2(\partial\Omega)$ -absolute error $\|\mathbf{X}_\nu - \tilde{\mathbf{X}}_\nu^{h_N}\|_{L_2(\partial\Omega)}$. In [Figure 3](#), we plot this L_2 -errors versus h_N (measured with

the Euclidean distance) for the kernels $k_4^{0.7}$, $k_6^{0.7}$, and $k_8^{0.7}$. The measured convergence rates read (approximatively) 4.20, 5.98, and 8.20 (when $h_N > 2^{-4}$), respectively. Similar compatible results are obtained for the nonconvex domain depicted in [Figure 1](#) (left), as well as for different values of σ . To interpret these results, let us first point out that $\tilde{\mathcal{R}}_N$ is only an approximation of \mathcal{R}_N . It may not be so simple to prove a proposition for $\tilde{\mathcal{R}}_N$ that is analogous to [Proposition 3.8](#), because $\tilde{\mathcal{R}}_N$ does not contain the image of the operator $\mathbf{X} \mapsto (\mathbf{X} \cdot \boldsymbol{\nu})\boldsymbol{\nu}$. Note also that it is true that $\mathbf{r}_x^{h_N}$ converges to \mathbf{r}_x as $h_N \rightarrow 0$, but [Theorem 2.32](#) does not guarantee that this convergence is uniform in \mathbf{x} . However, if we assume that a proposition analogous to [Proposition 3.8](#) exists for $\tilde{\mathcal{R}}_N$, we can explain the measured convergence rates with [10, Cor. 15], because interpolating a vector field \mathbf{f} into $\tilde{\mathcal{R}}_N$ or into $\mathcal{H}(\mathcal{X}_N) \times \mathcal{H}(\mathcal{X}_N)$ returns exactly the same interpolant if the vector field \mathbf{f} is normal to $\partial\Omega$.

Finally, the convergence history saturates for $k_8^{0.7}$ because the condition number of the discretised shape Hessian is very large for $N = 2^8$ (the MATLAB-function `cond` returns the value `4.826490e+18`). In a simple numerical experiment, we observed that the condition number of the discretised shape Hessian behaves as $h_N^{\alpha_h} \sigma^{\alpha_\sigma}$ with $\alpha_h = -8.7$ and $\alpha_\sigma = 7.2$ when $p = 4$ and $\alpha_h = -12.48$ and $\alpha_\sigma = 10.18$ when $p = 6$.

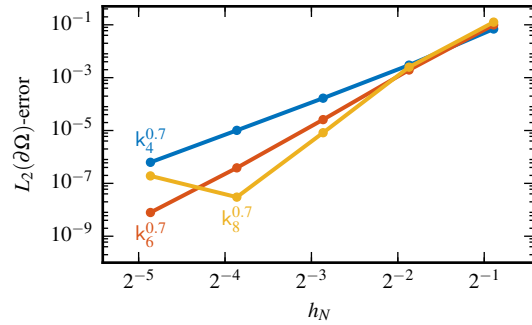


FIG. 3. [Numerical Experiment 3.9](#) shows that $\|\mathbf{X}_\nu - \tilde{\mathbf{X}}_\nu^{h_N}\|_{L_2(\partial\Omega)}$ decays with the algebraic rate 4.20 (for $k_4^{0.7}$), 5.98 (for $k_6^{0.7}$), and 8.20 (for $k_8^{0.7}$ when $h_N > 2^{-4}$).

3.3. Discrete shape Newton algorithm based on \mathbf{r}_x . In this section, we use the basis functions \mathbf{r}_x s to formulate a discrete shape Newton algorithm and test it on [Example 3.7](#). In particular, we investigate the impact of the Newton update approximation on the convergence rates of the shape Newton method. To measure these convergence rates, we use the norm on the tangent spaces, which is simply the norm of the RKHS.

Let J be a twice differentiable shape function, $\Omega \subset \mathbf{R}^2$ be an initial guess, and $\mathcal{X}_N = \{\mathbf{x}_1, \dots, \mathbf{x}_N\}$ be a finite number points on $\partial\Omega$. We begin by specifying how to transport the basis functions \mathbf{r}_x when Ω is perturbed by a geometric transformation.

DEFINITION 3.10. Let $\mathbf{r}_{\partial\Omega, \mathbf{x}}$ denote the weakly-normal function associated with $\partial\Omega$ and $\mathbf{x} \in \partial\Omega$, and let $F_t : \mathbf{R}^2 \rightarrow \mathbf{R}^2$ be family of C^1 -diffeomorphisms such that $F_0 = \mathbf{id}$. We define the transport \mathfrak{T}_s by

$$(90) \quad \mathfrak{T}_s(\mathbf{r}_{\partial\Omega, \mathbf{x}}) := \mathbf{r}_{F_s(\partial\Omega), F_s(\mathbf{x})},$$

and extend it by linearity to $\mathfrak{T}_s : \text{span}\{\mathbf{r}_{\partial\Omega, \mathbf{x}}, \mathbf{x} \in \partial\Omega\} \rightarrow \text{span}\{\mathfrak{T}_s(\mathbf{r}_{\partial\Omega, \mathbf{x}}), \mathbf{x} \in \partial\Omega\}$. By construction, $\mathfrak{T}_s : \text{span}\{\mathbf{r}_{\partial\Omega, \mathbf{x}}, \mathbf{x} \in \partial\Omega\} \subset [\mathcal{H}(\partial\Omega)]_\nu^2 \rightarrow [\mathcal{H}(F_t(\partial\Omega))]_\nu^2$.

Using this transport, we formulate the following discrete shape Newton method. Set $\Omega_0 = \Omega$, and $\tilde{\mathcal{R}}_N^0 := \text{span}\{\mathbf{r}_{\partial\Omega, \mathbf{x}}^h : \mathbf{x} \in \mathcal{X}_N\}$. The optimisation algorithm proceeds as follows: first, it computes the solution $\mathbf{g}_0 \in \tilde{\mathcal{R}}_N^0$ of

$$(91) \quad \mathfrak{D}^2 J(\Omega_0)(\mathbf{g}_0)(\boldsymbol{\varphi}) = -D J(\Omega_0)(\boldsymbol{\varphi}) \quad \text{for all } \boldsymbol{\varphi} \in \tilde{\mathcal{R}}_N^0;$$

then, it defines the transformation $F_0(\mathbf{x}) := \mathbf{x} + \mathbf{g}_0(\mathbf{x})$ and the new domain $\Omega_1 := F_0(\Omega_0)$; and finally, it defines the space $\tilde{\mathcal{R}}_N^1$ by transporting $\tilde{\mathcal{R}}_N^0$ with F_0 , that is,

$$(92) \quad \tilde{\mathcal{R}}_N^1 := \text{span}\{\mathbf{r}_{F_0(\partial\Omega), F_0(\mathbf{x})}^h : \mathbf{x} \in \mathcal{X}_N\}.$$

This procedure is repeated until convergence.

REMARK 3.11. *The shape Ω_1 that results by updating Ω_0 with \mathbf{g}_0 has the same regularity of \mathbf{g}_0 . Therefore, from a theoretical point of view, it may be necessary to regularise the update \mathbf{g}_0 to guarantee that [Assumption 2.8](#) remains fulfilled during the optimisation process. However, such a regularization is not necessary in practice when one employs the Wendland kernels from [Example 2.5](#). In this case, regularity is lost only at the points $\{\mathbf{x} \pm \sigma : \mathbf{x} \in \mathcal{X}_N\}$, whereas to construct the approximate weakly-normal function $\mathbf{r}_{\mathbf{x}}^h$ s it is necessary to evaluate $\boldsymbol{\nu}$ and $\boldsymbol{\tau}$ only at \mathcal{X}_N . Therefore, if $\{\mathbf{x} \pm \sigma : \mathbf{x} \in \mathcal{X}_N\} \cap \mathcal{X}_N = \emptyset$, the discrete algorithm does not perceive the loss of regularity of the domain.*

NUMERICAL EXPERIMENT 3.12. *We test this discrete shape Newton method by performing 5 optimisation steps to solve [Example 3.7](#) with $f(\mathbf{x}) = |\mathbf{x}|^2 - 1$ and*

$$(93) \quad \Omega = \{\gamma(\phi) = (0.2 + 1.15 \cos(\phi), 0.15 + 0.9 \sin(\phi)) : \phi \in [0, 2\pi)\}.$$

The (approximate) weakly-normal basis functions $\mathbf{r}_{\mathbf{x}}^h$ are constructed with the kernel $k_4^{0.7}$ on the sets

$$(94) \quad \mathcal{X}_N = \{\gamma(2\pi\ell/N) : \ell = 1, \dots, N\} \quad \text{with} \quad N = 2^4, 2^5, \dots, 2^8.$$

Following [18, 22], we neglect the curvature term in (82). In [Figure 4](#), we plot the evolution of the shape iterates $\{\Omega_\ell\}_{\ell=0}^2$ for $N = 2^4$ (top left) and for $N = 2^5$ (top right), and, for each N , we plot the values of the sequence $\{\|\mathbf{g}_\ell\|_{[\mathcal{H}]^2}\}_{\ell=0}^4$ (bottom left) and the measure of the quadratic rate of convergence $\{\|\mathbf{g}_{\ell+1}\|_{[\mathcal{H}]^2}/\|\mathbf{g}_\ell\|_{[\mathcal{H}]^2}^2\}_{\ell=0}^3$ (bottom right).

We observe that the sequence of shapes converges quickly to the minimiser (a circle of radius 1 centered in the origin), and that the discretisation error on the retrieved shape is not visible for $N \geq 2^5$. We also observe that the discretised shape Newton method converges quadratically, if sufficiently many weakly-normal vector fields are employed.

Finally, we have repeated the experiments including the curvature term in the Newton equation. Surprisingly, we observed that the convergence rates of the algorithm deteriorates drastically, although the sequence of shape iterates converge to the correct minimiser. Unfortunately, we cannot offer an explanation for this phenomenon.

4. Conclusion. In the first part of this work, we have introduced the class of weakly-normal vector fields, which are defined as solutions of saddle point variational problems in RKHSs. Besides investigating their properties, we have discussed their approximation and proved the related convergence rates. These vector fields can be

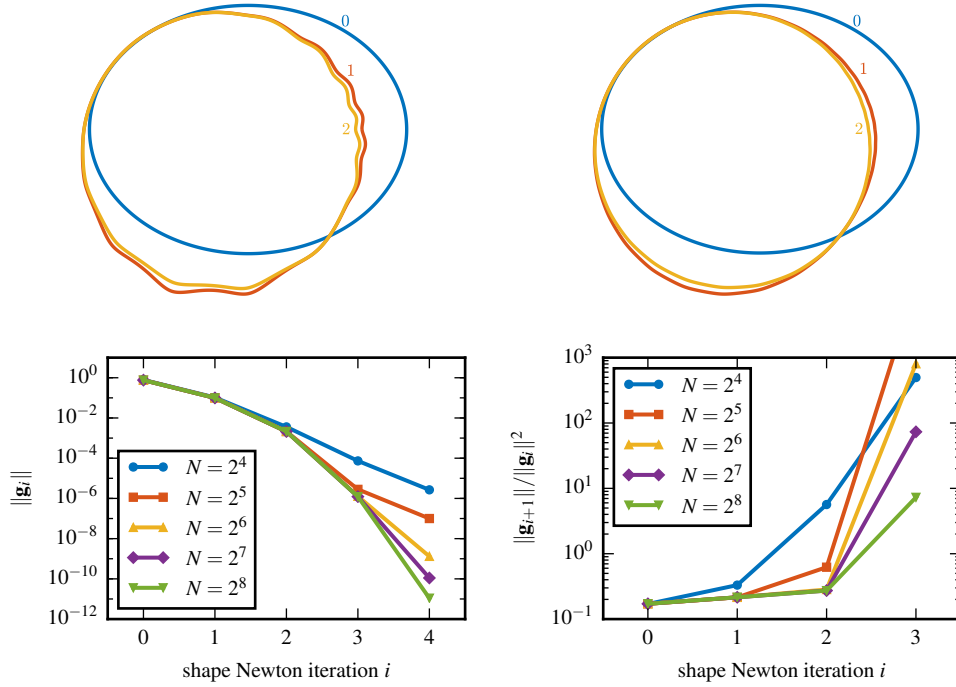


FIG. 4. *Numerical Experiment 3.12* shows that the discretised shape Newton method converges quadratically, if sufficiently many weakly-normal vector fields are employed.

used to discretise shape Newton methods because they have purely normal components.

In the second part of the work, we have formulated a discrete shape Newton method based on these weakly-normal vector fields and, for a specific test case, proved that the discrete shape Newton direction converges to the continuous one in the metric associated with the shape Hessian. Finally, we have showed that the discrete shape Newton method exhibits quadratic convergence if the discretisation error is sufficiently small.

The weakly-normal vector fields have another property that has not been exploited in this work: although defined on the boundary $\partial\Omega$, they can be straightforwardly extended to \mathbf{R}^2 . This implies that the discrete shape Newton method remains well-posed even when formulated with volume-based expressions of the shape derivative and the shape Hessian. This is a great advantage for PDE-constrained shape optimisation problems, in which case volume based formulas are easier to derive and impose less regularity requirements on the solution of the PDE-constraint. However, using volume-based formulas requires the integration of the weakly-normal vector fields on Ω , which introduces an additional complexity in the implementation as well as additional sources of discretization error that need to be analysed. For this reason, we postpone to a subsequent work the study of the shape Newton method based on weakly-normal vector fields in the framework of PDE-constrained shape functionals.

Appendix. In this appendix, we show that $\mathcal{H}(\partial\Omega) \subset C^0(\partial\Omega)$ when $k \in C^0(\mathbf{R}^2 \times \mathbf{R}^2)$. We believe that this result is not new, but we could not find its proof in the literature.

LEMMA 4.1. *Let k be a symmetric positive-definite kernel on \mathbf{R}^2 . Denote by $\mathcal{H}(\partial\Omega)$ the RKHS associated with the restriction of k to $\partial\Omega$. If $k \in C^0(\mathbf{R}^2 \times \mathbf{R}^2)$, then $\mathcal{H}(\partial\Omega) \subset C^0(\partial\Omega)$.*

Proof. For a generic $f \in \mathcal{H}(\partial\Omega)$, the reproducing kernel properties of $\mathcal{H}(\partial\Omega)$ implies

$$\begin{aligned} (95) \quad |f(\mathbf{x}) - f(\mathbf{y})| &= |(k(\mathbf{x}, \cdot), f)_{\mathcal{H}} - (k(\mathbf{y}, \cdot), f)_{\mathcal{H}}| \\ &= |(k(\mathbf{x}, \cdot) - k(\mathbf{y}, \cdot), f)_{\mathcal{H}}| \\ &\leq \|k(\mathbf{x}, \cdot) - k(\mathbf{y}, \cdot)\|_{\mathcal{H}} \|f\|_{\mathcal{H}} \end{aligned}$$

for all $\mathbf{x}, \mathbf{y} \in \partial\Omega$. Moreover,

$$(96) \quad \|k(\mathbf{x}, \cdot) - k(\mathbf{y}, \cdot)\|_{\mathcal{H}}^2 = k(\mathbf{x}, \mathbf{x}) + k(\mathbf{y}, \mathbf{y}) - 2k(\mathbf{x}, \mathbf{y}).$$

Therefore, the right hand side of (96) goes to zero as \mathbf{x} goes to \mathbf{y} because $k \in C^0(\mathbf{R}^2 \times \mathbf{R}^2)$. In view of estimate (95) and (64), this shows that f is continuous on $\partial\Omega$. \square

REFERENCES

- [1] G. ALLAIRE, E. CANCÈS, AND J.-L. VIÉ, *Second-order shape derivatives along normal trajectories, governed by hamilton-jacobi equations*, Structural and Multidisciplinary Optimization, 54 (2016), pp. 1245–1266.
- [2] D. BOFFI, F. BREZZI, AND M. FORTIN, *Mixed finite element methods and applications*, Springer, Heidelberg, 2013.
- [3] M. C. DELFOUR AND J.-P. ZOLÉSIO, *Velocity method and Lagrangian formulation for the computation of the shape Hessian*, SIAM J. Control Optim., 29 (1991), pp. 1414–1442.
- [4] M. C. DELFOUR AND J.-P. ZOLÉSIO, *Shapes and geometries: Metrics, analysis, differential calculus, and optimization*, Society for Industrial and Applied Mathematics (SIAM), Philadelphia, PA, second ed., 2011.
- [5] T. A. DRISCOLL, N. HALE, AND L. N. TREFETHEN, eds., *Chebfun Guide*, Pafnuty Publications, Oxford, 2014.
- [6] I. EKELAND AND R. TÉMAM, *Convex analysis and variational problems*, Society for Industrial and Applied Mathematics (SIAM), Philadelphia, PA, english ed., 1999.
- [7] K. EPPLER, *Second derivatives and sufficient optimality conditions for shape functionals*, Control Cybernet., 29 (2000), pp. 485–511.
- [8] K. EPPLER AND H. HARBRECHT, *A regularized Newton method in electrical impedance tomography using shape Hessian information*, Control Cybernet., 34 (2005), pp. 203–225.
- [9] K. EPPLER, H. HARBRECHT, AND R. SCHNEIDER, *On convergence in elliptic shape optimization*, SIAM J. Control Optim., 46 (2007), pp. 61–83.
- [10] E. FUSELIER AND G. B. WRIGHT, *Scattered data interpolation on embedded submanifolds with restricted positive definite kernels: Sobolev error estimates*, SIAM J. Numer. Anal., 50 (2012), pp. 1753–1776.
- [11] A. HENROT AND M. PIERRE, *Variation et optimisation de formes. Une analyse géométrique*, Springer, Berlin, 2005.
- [12] M. HINTERMÜLLER AND W. RING, *A second order shape optimization approach for image segmentation*, SIAM J. Appl. Math., 64 (2003/04), pp. 442–467.
- [13] LAURAIN, ANTOINE AND STURM, KEVIN, *Distributed shape derivative via averaged adjoint method and applications*, ESAIM: M2AN, 50 (2016), pp. 1241–1267.
- [14] A. NOVRUZI AND M. PIERRE, *Structure of shape derivatives*, J. Evol. Equ., 2 (2002), pp. 365–382.
- [15] W. RING AND B. WIRTH, *Optimization methods on Riemannian manifolds and their application to shape space*, SIAM J. Optim., 22 (2012), pp. 596–627.
- [16] R. SCHABACK, *Error estimates and condition numbers for radial basis function interpolation*, Adv. Comput. Math., 3 (1995), pp. 251–264.

- [17] A. SCHIELA AND J. ORTIZ, *Second order directional shape derivatives*, March 2017, <http://nbn-resolving.de/urn/resolver.pl?urn=urn:nbn:de:bvb:703-epub-3251-1>.
- [18] V. H. SCHULZ, *A Riemannian view on shape optimization*, Found. Comput. Math., 14 (2014), pp. 483–501.
- [19] V. H. SCHULZ, M. SIEBENBORN, AND K. WELKER, *PDE constrained shape optimization as optimization on shape manifolds*, in Geometric science of information, vol. 9389 of Lecture Notes in Comput. Sci., Springer, Cham, 2015, pp. 499–508.
- [20] V. H. SCHULZ, M. SIEBENBORN, AND K. WELKER, *Structured inverse modeling in parabolic diffusion problems*, SIAM J. Control Optim., 53 (2015), pp. 3319–3338.
- [21] J. SOKOŁOWSKI AND J.-P. ZOLÉSIO, *Introduction to shape optimization. Shape sensitivity analysis*, Springer, Berlin, 1992.
- [22] K. STURM, *Convergence analysis of newton’s method in shape optimization via approximate normal functions*, 2016, <https://arxiv.org/abs/1608.02699>.
- [23] H. WENDLAND, *Scattered data approximation*, Cambridge University Press, Cambridge, 2005.